

ROTORCRAFT WAKE VORTEX ENCOUNTERS: A FLIGHT MECHANICS PERSPECTIVE

B.Lawrence¹, G.D.Padfield², and A.Taghizad³

¹ Flight Science and Technology
Department of Engineering
University of Liverpool, Liverpool, L69 3GH, UK
e-mail: b.lawrence@liv.ac.uk

² Flight Science and Technology
Department of Engineering
University of Liverpool, Liverpool, L69 3GH, UK
e-mail: gareth.padfield@liv.ac.uk

³ System Control and Flight Dynamics Department
ONERA, Salon Research Centre, France
e-mail: Taghizad@onera.fr

Key words: Wake Vortex, Rotorcraft, Simulation

Abstract: The European Commission Framework VI project OPTIMAL is developing new rotorcraft and fixed-wing procedures to increase airport capacity, improve efficiency and reduce environmental impact. Among these procedures, the concept of rotorcraft Simultaneous Non-Interfering operations (SNIops) with heavy, runway-based fixed-wing traffic will feature. It has been identified that these operations present a potential risk for rotorcraft encountering the wake vortices of the fixed-wing aircraft. The research presented is part of an ongoing effort to understand the flight mechanics of a rotorcraft Wake Vortex Encounter (WVE) as well developing methods to assess the severity of a WVE. Models have been used in piloted simulation experiments and desktop simulations to include comparative studies of different rotorcraft configurations in a WVE. Parameters such as mass, rotor size, rotor speed and rotor stiffness have also been considered. This study also attempts to make the connection between a particular rotorcraft's sensitivity to a wake vortex and its basic design parameters through the use of flight stability and control derivatives. Results from piloted simulations will also be presented. The results build upon work presented at previous forums, incorporating new rotorcraft types and vortex encounter geometries. The paper presents results from the effort to create criteria for assessing severity and developing methods for linking the fast-time/offline simulation results to the piloted assessments. Establishment of such methods will allow the consideration of a greater number of configurations and scenarios, for example, in the development of safety cases for particular SNI proposals.

1 NOMENCLATURE

a_0	Blade lift curve slope [rad^{-1}]
a_x, a_y, a_z	X, Y, Z body-axes accelerations
Azb, azb	Z-axis (heave) body axis acceleration
\bar{A}	System state matrix
ACP	Aerodynamic Computation Point
ATM	Air Traffic Management
\bar{B}	Control Matrix
c	Blade chord
c.g.	Centre of gravity
C_D	Drag Coefficient
C_L	Lift Coefficient
C_M	Pitching Moment Coefficient
DVE	Degraded Visual Environment
e	Blade hinge offset (non-dimensional)
FATO	Final Approach and Take-Off area
g	Acceleration due to gravity
gs	glideslope
GVE	Good Visual Environment
h, \dot{h}	Height, height rate
H_{lat}	FATO distance from runway/taxiway
HQR	Handling Qualities Rating
h_R	Height of rotor hub above c.g.
ICAO	International Civil Aviation Organisation
ILS	Instrument landing System
IMC	Instrument Meteorological Conditions
IP	Integrated Project
I_{xx}, I_{yy}, I_{zz}	Roll, pitch and yaw moments of inertia
I_{xz}	Roll-yaw product of inertia
I_β	Blade flapping moment of inertia [slug-ft^2]
K_β	Rotor blade flapping stiffness [ft-lbf/rad]
LIDAR	Light Detection And Ranging system
$L_{\theta_{1s}}$	Rolling moment due to longitudinal cyclic Stability Derivative
$L_{\theta_{1c}}$	Rolling moment due to lateral cyclic Stability Derivative
MDH	Minimum Decision Height
M_{nd}	Non-dimensional mass $\frac{M}{\rho R^3}$
$M_{\theta_{1s}}$	Pitching moment due to longitudinal cyclic Stability Derivative i.e. $\frac{\partial M}{\partial \theta_{1s}}$
M_q	Pitching Moment due to pitch rate Stability Derivative
$N_{\theta_{0T}}$	Yawing moment due to tail rotor collective Stability Derivative
N_v	Yawing moment due to lateral velocity Stability Derivative
N_b	Number of rotor blades
OPTIMAL	Optimized Procedures and Techniques for Improvement of Approach and Landing
$\dot{p}, \dot{q}, \dot{r}$	Roll, pitch and yawing body-axes angular accelerations
p, q, r	Roll, pitch and yawing body-axes angular rates

Pdot or pdot	Roll angular accelerations
q_{ss}	Steady-state pitch rate
Qdot or qdot	Pitch angular accelerations
Rdot or rdot	Yaw angular accelerations
r_c	Vortex core radius
SNI or SNIops	Simultaneous Non-Interfering operations
S_β	Stiffness number $\frac{\lambda_\beta^2 - 1}{\gamma/8}$
T	Rotor thrust
v	Lateral (Body Y-axis) velocity
V_c	Vortex core tangential velocity
V_{linear}	Equivalent local blade downwash velocity for linear distribution
VMC	Visual Meteorological Conditions
VSR	Vortex Severity Rating
V_T	Vortex tangential velocity
V_{tip}	Equivalent downwash velocity computed at blade tip
VTOL	Vertical Take-Off and Landing
V_{vortex}	Local blade downwash velocity for actual vortex distribution
V_x	Body X-axis Velocity
WVE	Wake Vortex Encounter
XI	Inertial X position
YI	Inertial Y position
ZI	Inertial Z position
$zpos$	Vertical position of rotor hub with respect to vortex core
Z_{θ_0}	Vertical force due to collective Stability Derivative i.e. $\frac{\partial Z}{\partial \theta_0}$
α	Angle of attack of flow on blade section
ΔH	Height deviation
γ	Lock number $\frac{\rho c a_0 R^4}{I_\beta}$
Γ, Γ_0	Average vortex circulation
γ_h	Rotorcraft horizontal flightpath angle
Γ_r	Vortex circulation at a radial position r
θ	Helicopter pitch attitude
$\theta_{1s} \theta_{1c} \theta_0 \theta_{0t}$	Longitudinal cyclic, Lateral cyclic, Main rotor collective and Tail rotor collective
λ_β	Flap frequency ratio $\lambda_\beta^2 = 1 + \frac{K_\beta}{I_\beta \Omega^2} + \frac{eRM_\beta}{I_\beta}$
ρ	Density of air
Ω	Rotor angular speed
$\frac{\partial \beta_{1c}}{\partial \theta_{1s}}$	Blade longitudinal flapping due to longitudinal cyclic Stability Derivative
$\frac{\partial \beta_{1c}}{\partial q}$	Blade longitudinal flapping due to pitch rate Stability Derivative

2 INTRODUCTION

The ACARE (Advisory Council for Aeronautics Research in Europe) ‘2020 Vision’[1] predicts a near tripling of European air traffic. These pressures for greater airport capacity, improved efficiency, reduced environmental impact and increased safety are causing the aerospace community to look for new solutions. In response, the European Commission’s Framework VI project ‘OPTIMAL’ is developing one such set of solutions where it intends to ‘define and validate’ innovative procedures for the approach and landing phases of both aircraft and rotorcraft. The procedures will feature new trajectories using both new and existing precision landing aids as well as new Air Traffic Management technologies. Proposed within this framework are Simultaneous Non-Interfering rotorcraft operations. These operations will allow for a direct injection of rotorcraft into the airport terminal area thus increasing passenger throughput. Looking further into the future, it has been proposed that more capacity gains can be achieved by replacing short-haul turboprop aircraft with runway independent VTOL Tiltrotor aircraft [2]. The possibility of fully independent rotorcraft operations in the vicinity of larger fixed-wing aircraft requires consideration of the safe separation of the two types of traffic adding the issue of wake vortex separation between the traffic. Longitudinal separation for the protection against wake vortices has been in operation since the 1970’s with the standard ICAO weight-categorised separation rules (Figure 1).

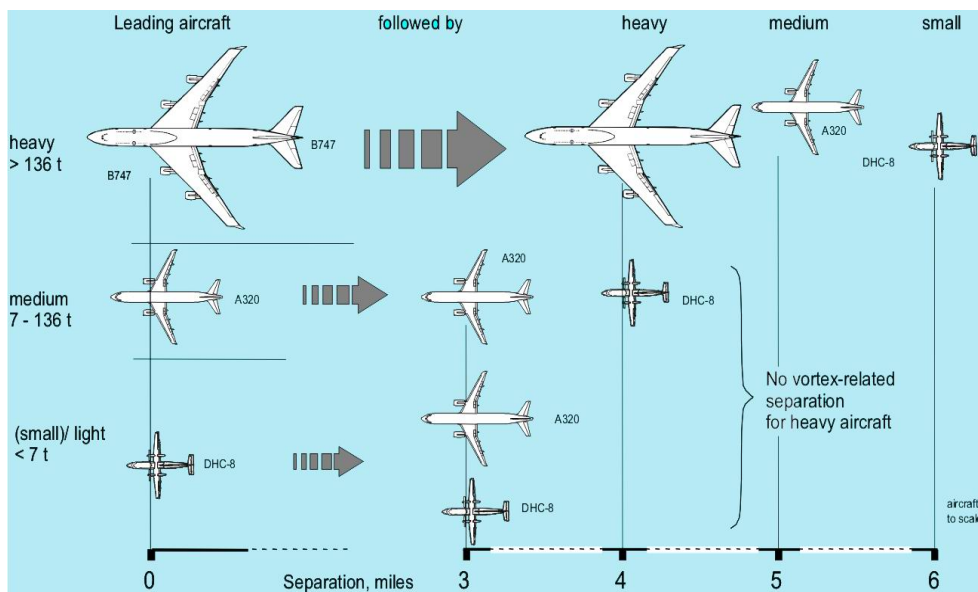


Figure 1 ICAO wake vortex separation distances

The premise is that the distances give sufficient separation on final approach such that the wake vortices of the lead aircraft have moved out of the flightpath of the following aircraft, or weakened enough that it is no longer a threat to safety. For simultaneous operations, the situation is more complex as it requires safe lateral separation as well as longitudinal separation. This is not only because of the adjacent operations, but because they are also independent and any positional combination of aircraft and rotorcraft is possible along their respective prescribed flightpaths. This means that wake vortex separation rules for SNI must consider the entire final approach flightpath and all wind vectors. Of course, the simplest solution to this problem is to ensure large separations of the traffic such that the possibility of an encounter is improbably remote. However, this requirement has a number of opposing constraints that vary with each airport. These include where the rotorcraft flightpaths can be placed within the ex-

isting traffic, local terrain and obstacle constraints, Final Approach and Take-Off area FATO (rotorcraft) and runway positioning constraints, and fly-over constraints (noise abatement). Once all these factors have been taken into account it is often quite difficult to select the 'ideal' positioning from a wake vortex separation point of view. These issues demand greater knowledge of the rotorcraft-wake vortex interaction. This includes not only understanding at the aerodynamics level but also in terms of the rotorcraft's overall response and how a pilot reacts to an encounter. Equipped with this knowledge, recommendations can be made for acceptable levels of risk of an encounter using a balance of the probability of encounter occurrence versus the likely severity.

How does one measure severity? This important question is one of the most critical issues for this study. A metric or measure is needed for quantifying how 'bad' or severe a particular encounter is or perhaps is likely to be. In the fixed-wing domain, criteria have been used or proposed with reasonable success including NASA's 'bank angle' [3] and a 'roll control' criterion [4]. The premise for these criteria is that the disturbance from a wake vortex encounter (WVE) is primarily a roll disturbance which is a reasonable simplification for conventional fixed-wing aircraft flying along parallel tracks. For rotorcraft, as this paper will show, the interaction is more complex and the disturbance is multi-axis. Furthermore, the proposed SNI operations allow for much more varying encounter geometries (i.e. parallel, crossing, oblique) especially as the new OPTIMAL procedures will feature steeper final approach glideslopes for rotorcraft (i.e. 6 degrees and possibly higher). All these factors change the nature of the wake encounter and this paper will demonstrate many aspects of this.

The amount of previous work in the area of rotorcraft wake vortex encounters is limited to handful of papers over 30 years. The research has arrived in three main waves with the first published work appearing in the late 1970's from Mantay, Holbrook *et al* [5]. Their work consisted of a series of papers presenting results from flight-tests using a Bell UH-1 helicopter attempting to fly into the trailing wake of C-54 aircraft. Various separation distances and intercept angles were tested and the main conclusions were that the helicopter's attitude responses were minimal with the yaw response being the most significant. Blade structural load perturbations were also adjudged not severe (less than those experienced in a 1.8g turn), and separation from the vortex generating aircraft did not affect the response strongly. All these results point to the response of a helicopter in a wake vortex from a generating aircraft of 58,000lbs to be fairly benign, especially if compared to the attitude responses that a fixed-wing aircraft of equivalent mass to the UH-1 (mass=3000kg, 6600lbs). The next 'wave' of research was published in 1986-87. Examples include Saito, Azuma *et al* [6-8] Their series of papers presented numerical simulations of various rotorcraft encountering B747 wakes of varying strengths. This work, like the previous references, included the UH-1 as a test rotorcraft but also featured the OH-6 (mass=1089kg, 2396lbs), a small light helicopter. The general conclusions were that the smaller helicopter suffered worse vertical accelerations, but perturbations were less than 2g. They also highlighted roll and yaw excursions as most dominant in parallel wake vortex encounters but for crossing or 'normal' encounters the vertical response was most significant. The most recent work initiated in the late nineties were from Padfield, Turner *et al* who published a number of papers studying various aspects of rotorcraft's response to a wake vortex. The first paper [9] featured FLIGHTLAB simulations of a Lynx in a B747 wake vortex. The paper considered the attitude and vertical displacements in a number of constrained low-speed encounters. One key development was the first connections made with handling qualities criteria. This paper was followed up soon after by further works considering more rotorcraft types and wake vortices [10, 11]. Various factors were investigated and the main findings included:

1. The pitch response was found to dominate in the parallel encounters not roll response as per fixed-wing encounters
2. The rotorcraft response is not as severe as for an equivalent fixed-wing aircraft as the blade loadings are much higher compared to a typical wing loading.
3. The severity was measured in terms of margins to the Handling Qualities (HQ) criteria charts, i.e. if a rotorcraft met a particular HQ level, what did this mean for its wake vortex encounter severity?
4. A SCAS tended to alleviate the rotorcraft's wake vortex response.
5. Reducing the encounter speed increased the time that the rotorcraft was exposed to the vortex resulting in larger attitude disturbances.

The latest paper also developed the analogy with handling qualities criteria and proposed a Vortex Severity Rating scale which is discussed later in this paper.

This paper will build upon previous reporting to the European Rotorcraft Forum, [12], continuing the severity criteria development work through piloted simulation. However, this paper also takes a step back with a more focussed look at the fundamental aeromechanics of a WVE. An analytical approach has been developed to synthesise the effect of a wake vortex. This has enabled a simpler, more understandable way to approximate the disturbance induced on a variety of helicopter-wake vortex combinations. Moreover, an attempt has been made to connect the severity ratings from the piloted simulations and the analytical model to correlate severity to a Vortex Parameter that defines a particular vortex-rotorcraft combination. Other work presented consists of the use of an autopilot model that flies a helicopter through a wake vortex. This analysis considers various encounter geometries and assesses the demanded control inputs required to maintain the helicopter on the desired trajectory.

3 SUMMARY OF SIMULATION AND MODELLING METHODS

As stated earlier, the work presented in this paper is a continuation of work presented in a previous paper [12]. The vortex model used was the 'Burnham' model [11] which specifies a tangential velocity distribution as a function of the radial location from the centre of the vortex. The Burnham model allows the entire velocity distribution to be defined using a nominal core radius, r_c and the core tangential velocity, V_c . Figure 2 shows a comparison of the velocity profile across a vortex core defined by the Burnham model to LIDAR measurements of actual B747 vortices.

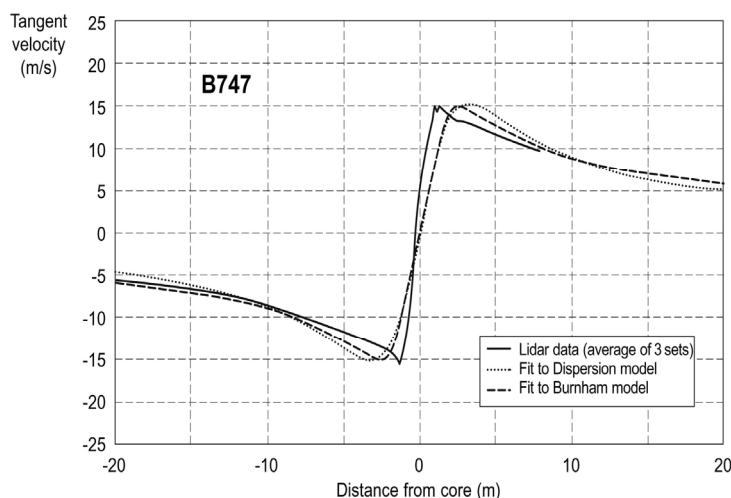


Figure 2 Velocity distribution in Boeing 747 Wake Vortex using the 'Burnham' model[11]

Table 1 shows a number of measured and estimated core radii and velocities for a variety of aircraft types that have been used for this analysis.

Aircraft	"Burnham" model	
	r_c (m)	V_c (m s ⁻¹)
B737-900 (estimated)	1.3125	11.25
B747	2.4	14.9
B757	<0.8	>21.2
A310	<1.0	>20
A340	2.0	11.4
DHC-8 (estimated)	1.0275	10

Table 1 Calculated and estimated Burnham model parameters for various full-strength vortices,[10]

In the FLIGHTLAB [13] environment, the wake vortex is modelled as a flow-field which has vertical and lateral velocity components (the axial component has been neglected) that varies with vertical and lateral coordinate. This means that the vortex flow-field is time-invariant and does not change due to any external effects (e.g. a helicopter wake etc) and is essentially a fixed 'tube' of rotating flow. The velocities of the vortex are picked up by the helicopter model at several 'airload computation points' (ACP's). Each ACP is a point where the aerodynamic incidence is computed and thus aerodynamic forces act. Typically, there are five ACP's per rotor blade (20 for a 4-bladed rotor), one on the fuselage, one for the tail rotor and one each for the vertical fin and empennage. The velocities are then applied to the helicopter using the principle of superposition i.e. the wake vortex velocity vectors are added to the other flow and kinematic velocities.

A number of FLIGHTLAB rotorcraft models have been used for the analysis in this paper –all are of a 'medium' fidelity level, featuring blade-element main rotors with quasi-steady, non-linear lift, drag and pitching moment data for each blade segment. The models also have separate fuselage, fin and empennage models, 3 or 4-state dynamic inflow models and Bailey or ducted-fan tail rotor models. The models also feature engine and control system models of varying complexity. For the piloted simulation, the models that have been mainly used are the AS365N Dauphin and the FLIGHTLAB Generic Rotorcraft (FGR) which approximates to the UH-60 Blackhawk. These two models represent two classes of helicopters with masses of around 3500kg and 7500kg respectively. However, to investigate more types, FLIGHTLAB models of the Bell-412, Lynx and Bo-105 helicopters have also been used.

4 DEVELOPMENT OF SIMPLIFIED ANALYTICAL WAKE VORTEX MODEL

The objective of this aspect of the wake encounter study is to develop a method for relating encounter 'parameters' to the severity of the wake encounter. The goal is that the complex flow-field of a vortex can be represented more simply as an 'equivalent' control input such as cyclic or collective. As such, the disturbances are more readily applicable for use in conjunction with the stability derivatives of a particular rotorcraft. This allows prediction of the 'sensitivity' of the rotorcraft to a particular vortex in terms of the acceleration, rate, attitude or displacements induced. Furthermore, the derivatives themselves are a function of the rotorcraft configuration, such as mass, inertia, rotor radius, Lock number, rotor stiffness etc. This

paves the way for defining the fundamental ‘rules’ for the flight dynamic effect of a particular vortex with certain rotorcraft design parameters. If a connection can then be made back to piloted simulation and the severity criteria, then a relationship could be made between rotorcraft configuration and probably severity.

4.1 Peak pitch acceleration scenario (parallel flightpath)

The first challenge was to compute an equivalent control input from the wake vortex flow field. The concept stems from work in [10] where the transverse distribution of vertical velocity that a vortex imposes on a rotor (when the hub is at the centre of the vortex core) was shown to be analogous to a linear velocity distribution across the rotor disc. The linear velocity distribution can be interpreted as an equivalent cyclic pitch input. In fact, the 90° phase shift effect of a rotor means that the lateral velocity distribution is equivalent to a longitudinal cyclic pitch input (Figure 3). The acceleration or force/moment induced can then be computed via the cyclic angle multiplied by the appropriate control derivatives.

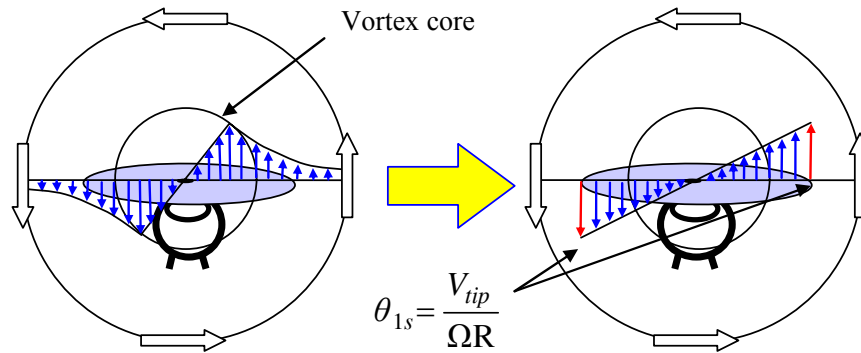


Figure 3 Equivalence of the vortex wake induced vertical velocity to a linear velocity distribution

In order to calculate the velocity distribution correctly there is the requirement to achieve an equivalent blade moment. The moment perturbations are given by the lift perturbation distribution along the blade multiplied by the radial distance (Equation 1). The lift distribution itself is a function of the radial incidence and dynamic pressure distribution [9] (Equation 2). For the analytical model, the simplification has been made the rotor has a ‘centre-spring’ model with an equivalent stiffness to represent the hinge offset. The aerodynamic moment therefore is integrated from the rotor centre to the blade tip.

$$\int_0^R L_{linear}(r)rdr = \int_0^R L_{vortex}(r)rdr \quad (1)$$

The lift along the blade is a function of the local velocity and incidence, taking the simplest case of the hover to start:

$$\int_0^R \frac{1}{2} \rho (\Omega r)^2 SC_L(r) r dr = \int_0^R \frac{1}{2} \rho (\Omega r)^2 SC_L(r) r dr$$

where $(V_{vortex/linear}(r)) \ll \Omega r$ and

$$\left[C_L(r) = C_{L\alpha} \alpha(r) \right] \quad \text{and} \quad \left[\alpha(r) = \frac{V_{linear/vortex}(r)}{\Omega r} \right]; \quad (2)$$

$$\int_0^R \frac{1}{2} \rho (\Omega r)^2 SC_{L\alpha} \frac{V_{linear}(r)}{\Omega r} r dr = \int_0^R \frac{1}{2} \rho (\Omega r)^2 SC_{L\alpha} \frac{V_{vortex}(r)}{\Omega r} r dr$$

Cancelling the constants on each side of the expression:

$$\int_0^R \Omega r^2 \frac{V_{linear}(r)}{r} r dr = \int_0^R \Omega r^2 \frac{V_{vortex}(r)}{r} r dr \quad (3)$$

$$\int_0^R (V_{linear}(r)) r^2 dr = \int_0^R (V_{vortex}(r)) r^2 dr$$

Substituting expressions for the velocity profiles gives:

$$\left[V_{linear}(r) = V_{tip} \frac{r}{R} \right];$$

$$\left[V_{vortex} = V_c \frac{r}{r_c} \right] \quad (r < r_c)$$

$$\left[V_{vortex} = V_c \left\{ 1 + \ell n \frac{r}{r_c} \right\} \frac{r_c}{r} \right] \quad (r > r_c) \quad (4)$$

$$\int_0^R \left(V_{tip} \frac{r^3}{R} \right) dr = \int_0^{r_c} \left(V_c \frac{r^3}{r_c} \right) dr + \int_{r_c}^R \left(V_c \left\{ 1 + \ell n \frac{r}{r_c} \right\} r_c r \right) dr$$

Evaluating the integrals:

$$V_{tip} \frac{R^3}{4} = V_c \frac{r_c^3}{4} + \left[V_c r_c \left[\left\{ 1 + \ell n \left(\frac{r}{r_c} \right) \right\} \frac{r^2}{2} - \frac{r^2}{4} \right] \right]_{r_c}^R \quad (5)$$

Thus using the example of the Dauphin helicopter in a Boeing 747 vortex (rotor radius=19.57ft, $r_c=8.235$ ft and $V_c=52.49$ ft/s), V_{tip} , the velocity calculated, is 60.33ft/s or 18.38 m/s. The equivalent cyclic input can be calculated by the increment in incidence at the blade tip:

$$V_{tip} = 60.3258 \text{ ft/s}; \quad \Omega = 36.65 \text{ rad/s}; \quad R = 19.57 \text{ ft}$$

$$\theta_{1s} = \frac{V_{tip}}{\Omega R} = \frac{60.3258}{717.24} = 0.0841 \text{ radians or } 4.82 \text{ deg} \quad (6)$$

To test this hypothesis, two cases were compared using the non-linear FLIGHTLAB model. The first is for the Dauphin helicopter model placed with the hub at the vortex core (as close as possible to represent the situation in Figure 3). The response of the helicopter in pitch was then recorded. To simplify the scenario all the other axes were ‘frozen’ meaning that the simulation was essentially 1-degree-of-freedom (although all rotor states were still free). The second cases is for the same model, with the same constraints, except that instead of a vortex, the ‘equivalent’ longitudinal cyclic pitch was applied. Figure 4 shows the comparison.

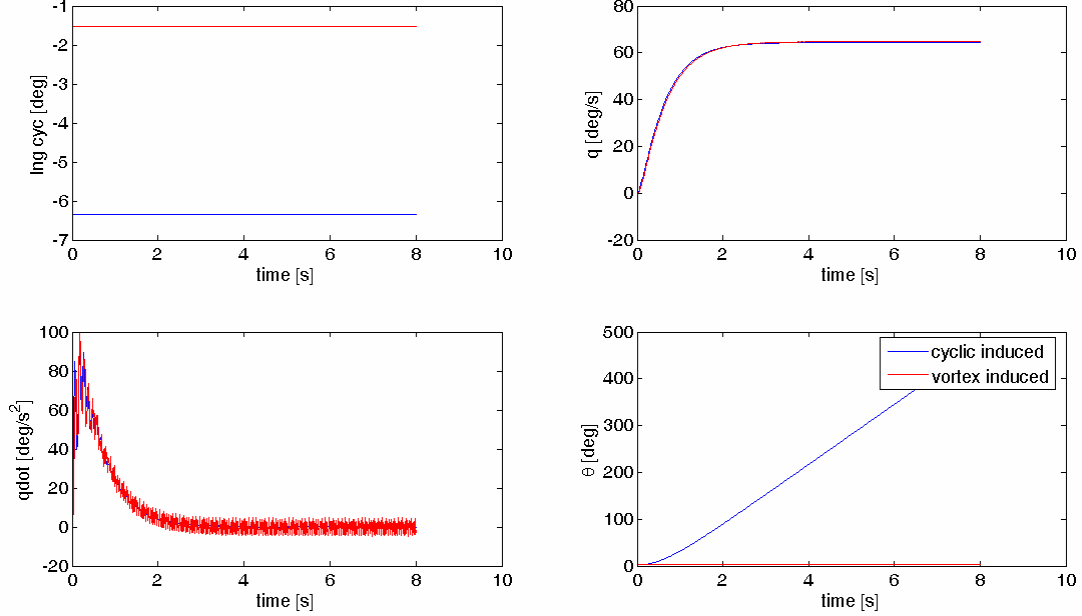


Figure 4 Comparison of the pitch rate perturbations induced by a wake vortex and the ‘equivalent’ longitudinal cyclic input of -4.81 degrees (-0.0841 radians) for the FLIGHTLAB non-linear AS365N Dauphin model

It can be seen that in this simple test there is a good agreement for the pitch response. However for the response within the vortex, the pitch attitude was also artificially constrained so that the flow field on the disc was constant (i.e. the integration of the pitch rate was still computed). In reality, as the helicopter pitches the vortex flow-field would have changed with respect to the rotor disc. Taking the concept one step further, it is possible to predict the induced acceleration and the theoretical peak steady-state rate response to the vortex based on the linear derivatives. First, considering the pitch response to the vortex, the key stability derivatives are $M_{\theta_{1s}}$ and M_q . From these it is possible to calculate the peak pitch acceleration, \dot{q} and the theoretical steady state pitch rate, q_{ss} from the following expressions[14]:

$$\dot{q} = M_{\theta_{1s}} \theta_{1s} \quad (7)$$

$$q_{ss} = \frac{M_{\theta_{1s}}}{M_q} \theta_{1s} \quad (8)$$

$$M_{\theta_{1s}} = -\left(\frac{N_b}{2} K_\beta + h_R T\right) \frac{\partial \beta_{1c}}{\partial \theta_{1s}} \quad (9)$$

$$M_q = -\left(\frac{N_b}{2} K_\beta + Th_R\right) \frac{\partial \beta_{1c}}{\partial q} \quad (10)$$

Using equations 7-10, the results in Figure 5 were obtained that show a comparison of the pitch acceleration calculated by the non-linear FLIGHTLAB rotorcraft model in the vortex, the equivalent longitudinal cyclic applied to the non-linear model, and the approximate analytical model.

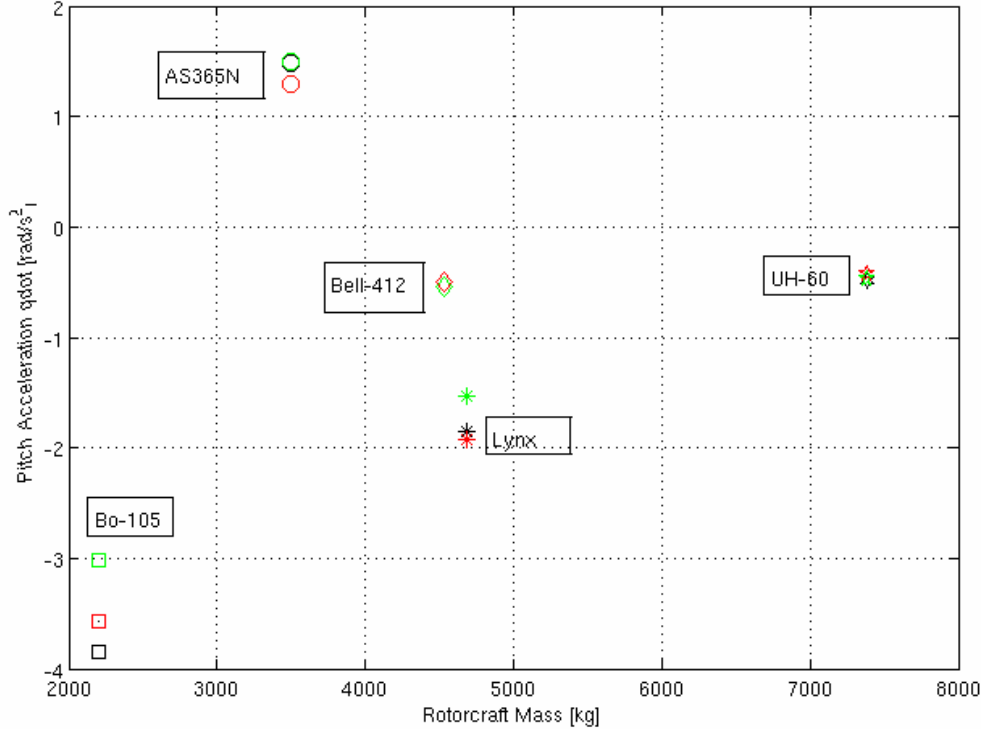


Figure 5 Comparison of the analytical wake vortex mode (green) pitch acceleration and the non-linear FLIGHTLAB model in the wake vortex (red) with the equivalent cyclic input (black). All the rotorcraft have the rotor hub in the vortex centre and are in the hover.

The results show that the analytical model is fairly successful at predicting the pitching acceleration for a variety of rotorcraft types. For the two rotorcraft with hingeless rotor systems (Lynx and Bo-105), the agreement is less well predicted but the overall trends are still followed.

4.2 Peak roll, yaw and heave acceleration scenarios

The success of predicting the pitch acceleration led to the consideration that the same methodology could be used to predict the peak accelerations in the heave (vertical axis), roll and yaw axes. Figures 6-10 show contour plots for the various rotorcraft in a B747 vortex pair, the vortex cores are at the vertical coordinate=0 and at ± 86.7 ft. The plots represent a quasi-steady scenario where the helicopter has been ‘frozen’ within the vortex at various locations and the ‘steady-state’ accelerations have been ‘measured’ (averaged over a rotor revolution). This tool allows the rotor dynamics to remain free and the contours show that the peak ‘initial’ accelerations occur at different locations within the flow-field [15]. It must be stated at this point that although the ‘checks’ presented in figures 4 and 5 were in the hover, the methodology is applicable to all speeds. The speed sets the trim condition (and thus the derivative values) upon which then the vortex effect is ‘superimposed’ via the equivalent control.

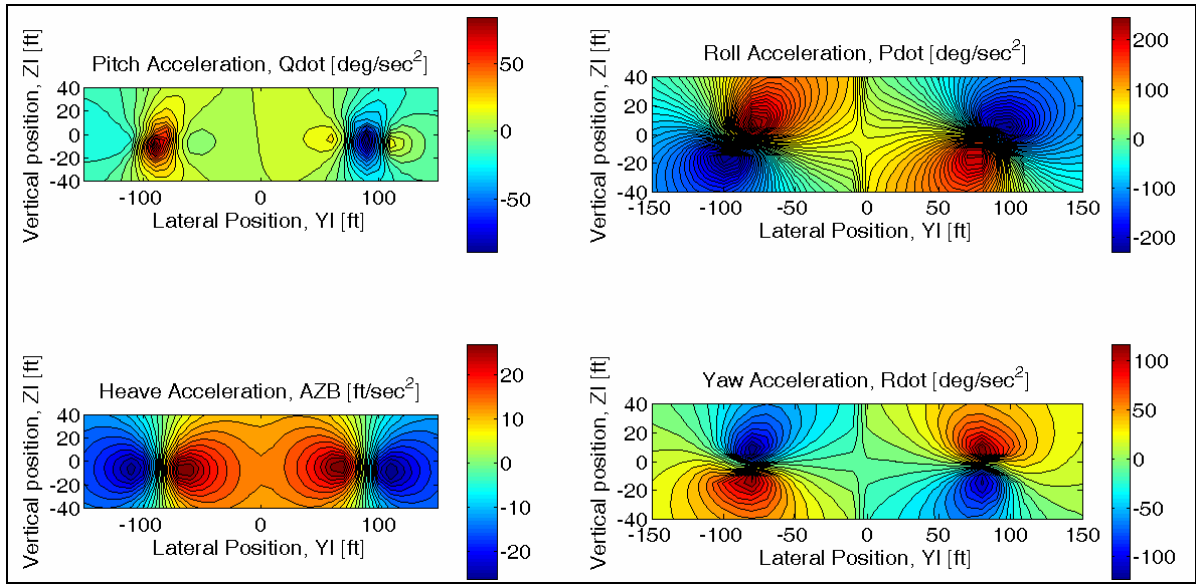


Figure 6 Steady-state Acceleration contours, AS365N 70kts, parallel encounter, B747 vortex pair

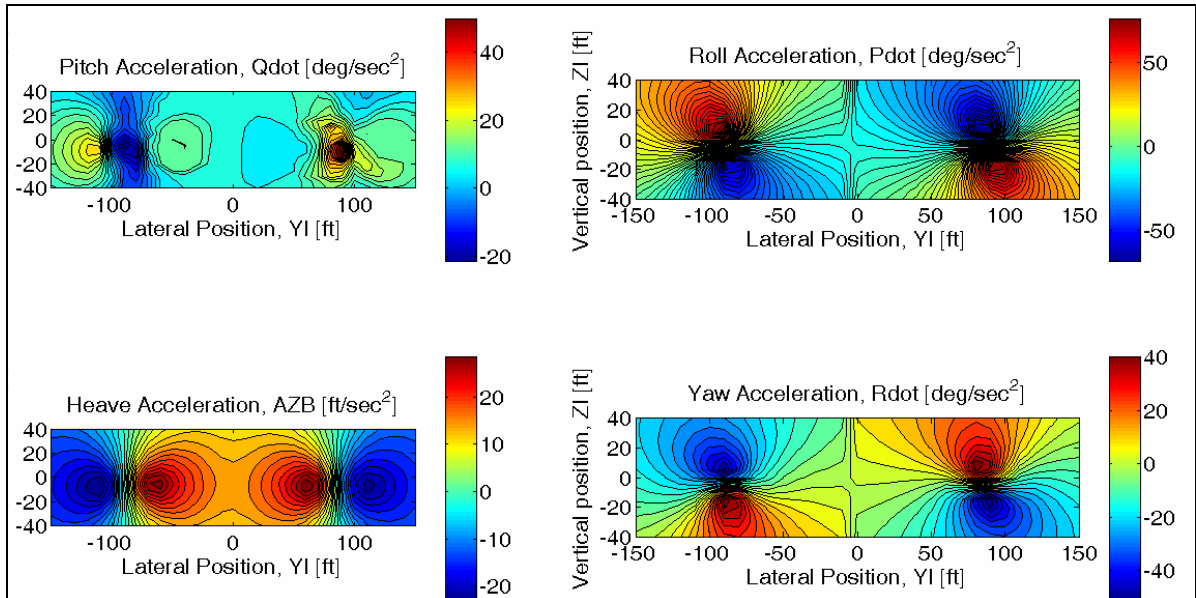


Figure 7 Steady-state Acceleration contours, Bell-412 70kts, parallel encounter, B747 vortex pair

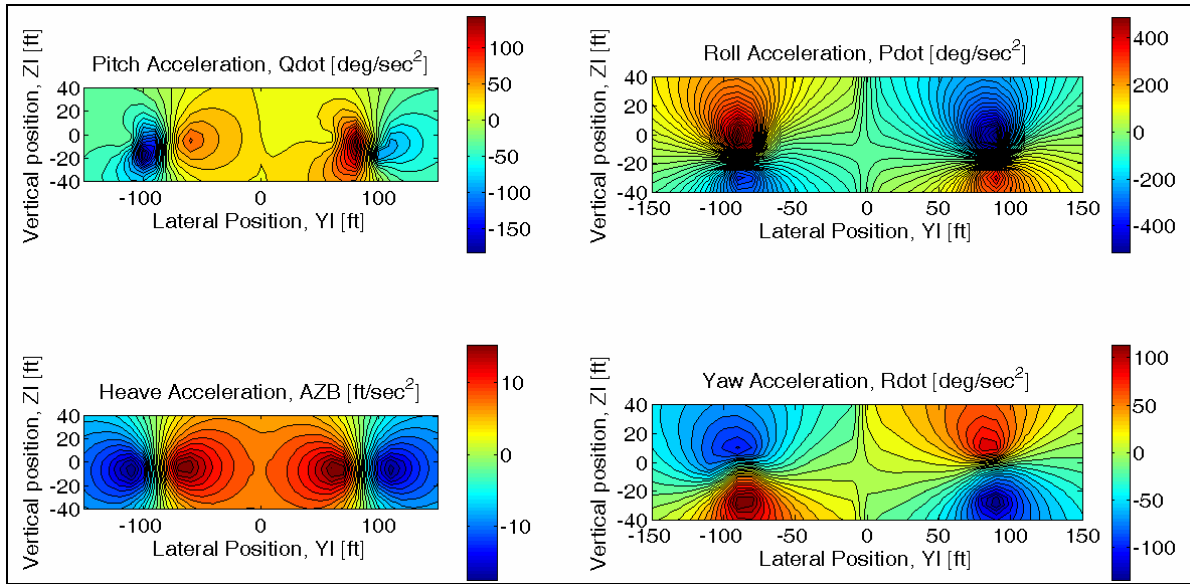


Figure 8 Steady-state Acceleration contours, Lynx 70kts, parallel encounter, B747 vortex pair

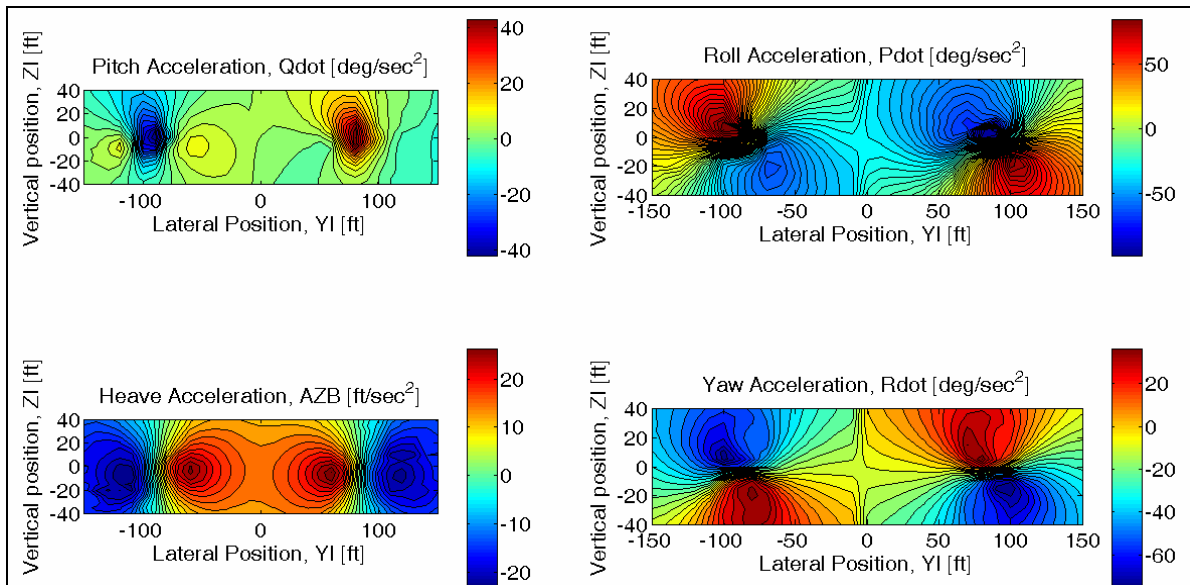


Figure 9 Steady-state Acceleration contours, FGR, 70kts, parallel encounter, B747 vortex pair

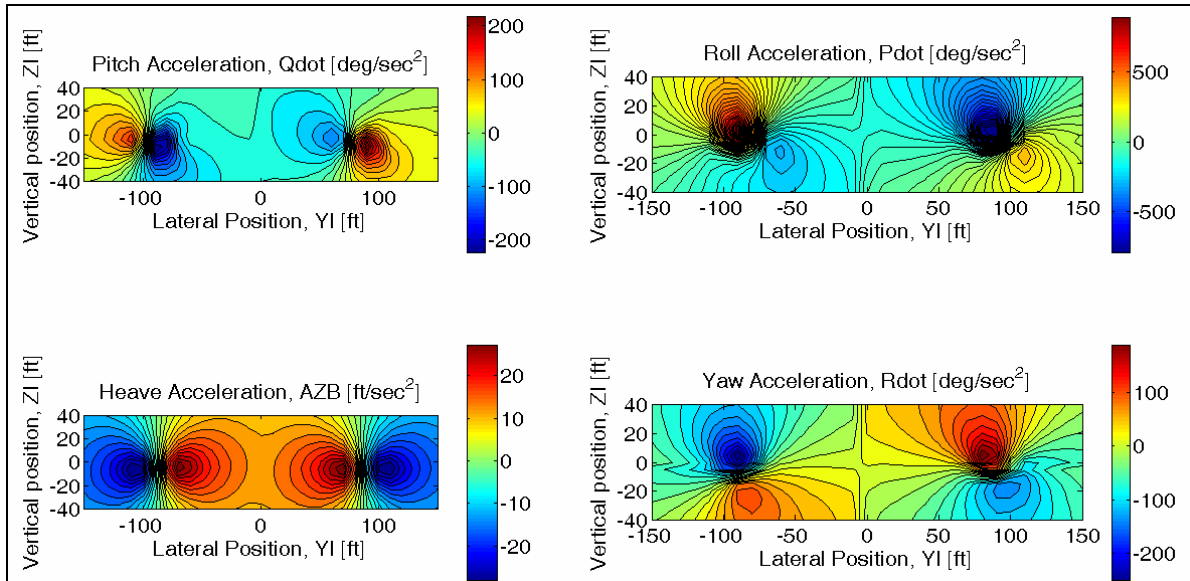


Figure 10 Steady-state Acceleration contours, Bo-105 70kts, parallel encounter, B747 vortex pair

The peak pitch acceleration occurs at the vortex core centre (top-left plot of Figures 6-10) and changes in direction depending on the rotation of the vortex (and rotor). The peak roll accelerations occur at locations where the rotor disc is approximately at top and bottom ‘edges’ of the core. At this location, there is a flow across the disc (in plane of the rotor) causing the blade to flap up on one side of the disc and down on the opposite side as per a lateral cyclic input. In addition to this, some rolling acceleration is induced by the vertical flow distribution across the disc. It has already been shown that this causes a pitching moment. However, this distribution also induces a rolling moment via the rotor’s pitch-roll coupling - the stiffer the rotor, the greater the coupling. This is the cause for the differences in the roll acceleration contours for the different rotorcraft. It can be seen that for most of the helicopters the roll acceleration reverses sign above and below the vortex core and is approximately of equal magnitude. However, for the rotorcraft with hingeless rotors such as the Lynx and Bo-105, the strength of the acceleration above the core is much higher than below. In fact, for the Bo-105, the contour is more like the pitch axis with the main peak near to the core centre, except the region of high roll acceleration extends somewhat upwards from it. The mechanism for how this occurs is illustrated in Figure 11:

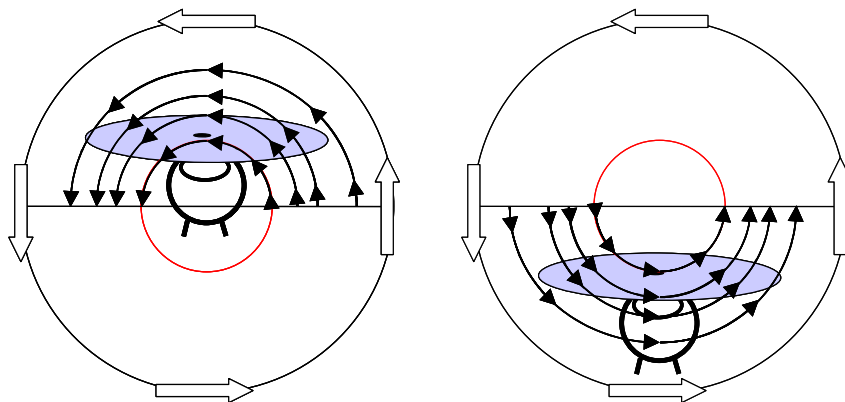


Figure 11 Schematic showing the airflow effect that causes the peak rolling acceleration

From Figure 11 it can be seen that circulatory flow causes both upwash on either side of the rotor disc and a lateral flow across the disc. The cause of the roll acceleration asymmetry is

therefore as follows: Above the core, the equivalent lateral cyclic caused by the in-plane lateral flow and the roll acceleration due to the pitch-roll coupling effect act together in the same direction. However, moving to below the core, the vertical velocity distribution remains essentially the same (upwards on the viewer's right, downwards on left) but the lateral flow reverses in direction. This causes the two components of the roll acceleration to now act against each other. For the Bo-105, the pitch-roll coupling is so strong that it dominates, such that roll acceleration below the core is much weaker than above. The Lynx is similar but its rotor is slightly less stiff, and the effect is less overpowering. The coupling is much weaker for the remaining rotorcraft, and thus the in plane flow effect is more significant, and the roll acceleration tends to reverse as the rotorcraft moves vertically through the core.

To calculate the roll acceleration, the equivalent vertical downwash is integrated to give an equivalent longitudinal cyclic, θ_{1s} . However, in this case, the coupling derivative is used to calculate the induced rolling acceleration. The expressions to obtain the equivalent longitudinal and lateral cyclic angles are shown in equations 11 and 12.

$$\int_0^R \left(\frac{V_{tip} r^3}{R} \Omega \right) dr + \int_0^R \left(\frac{V_{tip}^3 r^3}{\Omega R^3} \right) dr = \int_{r_c}^R \left(V_c r \left\{ 1 + \ln \left(\frac{\sqrt{r^2 + zpos^2}}{r_c} \right) \right\} \frac{r_c}{(r^2 + zpos^2)} \Omega r^2 \right) + \int_{r_c}^R \left(V_c r \left\{ 1 + \ln \left(\frac{\sqrt{r^2 + zpos^2}}{r_c} \right) \right\} \frac{r_c}{(r^2 + zpos^2)} \right)^3 \frac{1}{\Omega} dr \quad (11)$$

$$\int_0^R \left(\Omega r^2 + \frac{V_{tip}^3 r^3}{\Omega R^3} \right) dr = \int_0^R (\Omega r^2 + V_c r) dr \quad (12)$$

$$\dot{p} = L_{\theta_{1s}} \theta_{1s} \quad (13)$$

This is added to the in-plane flow contribution which has an equivalent lateral cyclic given in the expression

$$\dot{p} = L_{\theta_{1c}} \theta_{1c} \quad (14)$$

Thus, the total expression for the rolling acceleration is given by

$$\dot{p} = L_{\theta_{1c}} \theta_{1c} + L_{\theta_{1s}} \theta_{1s} + \dot{r} \begin{pmatrix} I_{xz} \\ I_{xx} \end{pmatrix} \quad (15)$$

Note that there is also an inertia coupling term from the yaw acceleration. This term is not usually significant as the yaw acceleration is often significantly smaller than the roll acceleration and/or the cross-product of inertia I_{xz} is usually much smaller than the roll inertia I_{xx} . However, there are some exceptions such as the Lynx.

As can be seen from Figures 6-10, the peak vertical or heave acceleration occurs when the rotorcraft is either side of the core and is in the region of maximum up-wash or downwash. As with the roll and pitch cases, this disturbance can be approximated by an equivalent linear velocity distribution and thus to an equivalent control input. From inspection of the contour

plots it appears that peak load occurs when the rotor was positioned relative to the core as shown in Figure 12.

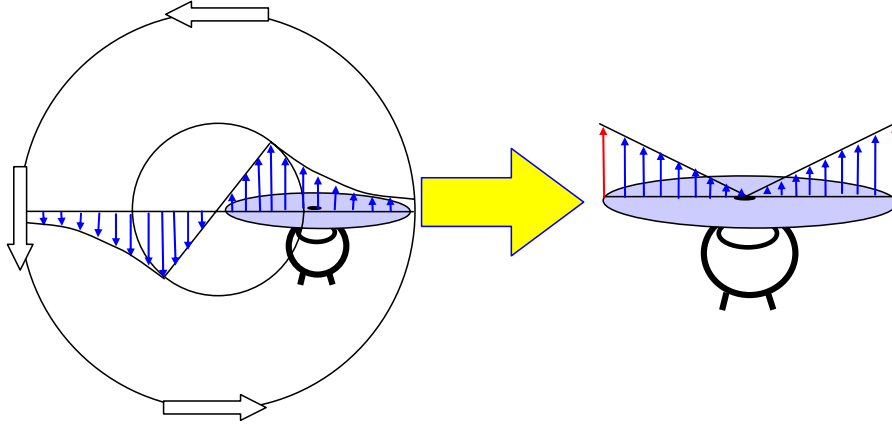


Figure 12 Equivalent linear velocity flow field for a collective input –peak vertical acceleration scenario

To achieve an equivalent vertical response the obvious choice of control input is an equivalent collective input. When a collective input is applied it increases the angle of incidence by a constant amount along the blade. The velocity distribution to imitate this effect is shown in Figure 12. By integrating the vortex velocity flow-field across the disc diameter, the equivalent velocity is calculated to give the equivalent lift force. The expression used to calculate this is shown in equation 16.

$$\int_0^{2R} V_{tip}^3 (\Omega|r-R|) dr + \int_0^{2R} V_{tip} \left(\frac{1}{(\Omega|r-R|)} \right) dr = \int_0^{r_c} \left(V_c \frac{(|r-R|\Omega r)}{r_c} \right) dr + \int_0^{r_c} \left(V_c \frac{r}{r_c} \right)^3 \left(\frac{1}{\Omega(|r-R|)} \right) dr \quad (16)$$

$$+ \int_{r_c}^{2R} \left(V_c \left\{ 1 + \ell n \frac{r}{r_c} \right\} \frac{r_c}{r} \right) (\Omega|r-R|) dr + \int_{r_c}^{2R} \left(V_c \left\{ 1 + \ell n \frac{r}{r_c} \right\} \frac{r_c}{r} \right)^3 \left(\frac{1}{\Omega(|r-R|)} \right) dr$$

In this case, the integration limits are 0 to 2R because the vortex downwash across the disc is not symmetric about the hub. The modulus of the radial distance also has to be used to account for the blade local velocity variation from one tip through the hub to the other side of disc. Once the equivalent tip velocity has been calculated, the equivalent collective, θ_0 can be obtained in the same method as used in equation 6. Finally, to calculate the peak acceleration, the control derivative, Z_{θ_0} is used:

$$\dot{w} = Z_{\theta_0} \theta_0 \quad (17)$$

The peak yaw acceleration usually occurs at about the same location as the peak roll acceleration –just above and below the vortex core. This is due to two main factors; the first is that the tail rotor and vertical fin experience a cross-flow that causes a weathercock effect i.e. if the flow is left to right, then the rotorcraft will experience a negative (nose left) yawing acceleration. The second factor is that the inertia coupling can be significant if the rolling acceleration is very large. Another contribution can come from the torque effect of changing the rotor loading when the rotor is the vertical flow. The yaw is a difficult axis to assess as there are a number of effects to consider including strong non-linearity in the behaviour of the key de-

ivative N_v [14] – the full expression for the calculation of the yaw acceleration is shown in equation 18.

$$\dot{r} = N_v v + \dot{p} \frac{I_{xz}}{I_{zz}} + N_{\theta_0} \theta_0 \quad (18)$$

For this expression the sway velocity, v can be assumed equal to V_c , and the term θ_0 represents the equivalent collective input for the vertical loading of the disc in the vortex, this would be obtained in a similar procedure as the ‘equivalent collective method’ described earlier in this paper.

4.3 Using the analytical model to develop the ‘Vortex Parameter’ concept

Figures 13-15 show the some of the acceleration predictions achieved with the simplified wake vortex model. What is shown are the peak pitch, roll and heave accelerations for a number of rotorcraft-wake vortex combinations. It must be reiterated that these figures are only valid for the parallel encounter (i.e. the rotorcraft flies along the rotational axis of the vortex) and that the peak accelerations are due to the aerodynamic loads only. For each axis, the computed result is plotted against a ‘Vortex Parameter’, which varies for each axis and is shown in equations 20-22.

$$\text{Pitch acceleration Vortex Parameter:} \quad V_c \frac{2\pi \left(\frac{r_c}{R} \right)}{\left(r_c^2 + R^2 \right)} \left(\frac{S_\beta}{1 + S_\beta^2} \right) \gamma \left(\frac{\rho R^5}{I_{yy}} \right) \quad (20)$$

$$\text{Roll acceleration Vortex Parameter:} \quad V_c \frac{2\pi \left(\frac{r_c}{R} \right)}{\left(r_c^2 + R^2 \right)} \left(1 + \exp\left(\frac{r_c}{R} \right) \right) \left(\frac{R}{r_c} \right) \left(\frac{S_\beta (1 - S_\beta^2)}{1 + S_\beta^2} \right) \left(\frac{\rho R^5}{I_{xx}} \right) \quad (21)$$

$$\text{Vertical acceleration Vortex Parameter:} \quad V_c \left(\frac{1}{BL} \right) \left(1 + \exp\left(\frac{r_c}{R} \right) \frac{r_c}{R} \right) \quad (22)$$

These parameters represent an attempt to ‘collapse’ the accelerations into single linear trends thus giving a measure for a particular rotorcraft-wake vortex combination. It can be seen that reasonable linear trends are achieved within the scatter of the results. The methods used to obtain the Vortex Parameter were fairly simplistic; for the roll and pitch axes, the parameter was assumed to need several contributions to capture the necessary effects. There was a need to reflect the ‘size’ of the rotorcraft – in this case the non-dimensional roll or pitch inertia was used, and for the rotor itself, the stiffness and radius needed to be incorporated. It can be seen that the rotor radius, R appears several times in the expressions reflecting the complex interdependency of the radius of the rotor on the overall induced acceleration. Also, it was necessary to include a factor to reflect the vortex strength. At first, the non-dimensional circulation was used, as shown below:

$$\frac{\Gamma}{\Omega R^2} \quad (19)$$

However, when used within the Vortex Parameter this did not give good correlations with the computed accelerations. Due to the non-linear velocity distribution across the vortex it was found that a better correlation was achieved using a proportional relationship with the vortex core tangential velocity, V_c . The different mechanisms for the generation of the pitch and roll

accelerations meant that the effect of the flow distribution was more difficult to identify. For the pitch axis, the rotor is across the centre of the vortex core and the main mechanism is the vertical flow across the disc so a parameter adapted from the ‘Dispersion’ [9] wake vortex model was used. It was expected that this would capture the relationship between the rotor radius and vortex core size. The Dispersion model was selected as it was able to provide a velocity distribution from the core centre to infinity in one expression. The roll axis also uses this parameter, as the same mechanism, albeit weaker, via the pitch-roll coupling, has a contribution to the induced roll acceleration. However the roll acceleration is also dependent on the cross flow component that is accounted for with extra terms. The trends for both the pitch and roll accelerations are to be expected, with the Bo-105 experiencing the greatest effect due to its combination of a stiff rotor and low inertia. Generally speaking, as the rotorcraft become larger, the inertias become larger, thus the induced accelerations reduce. The smallest effect is seen for the FGR (UH-60) which has a relatively soft rotor and high inertias.

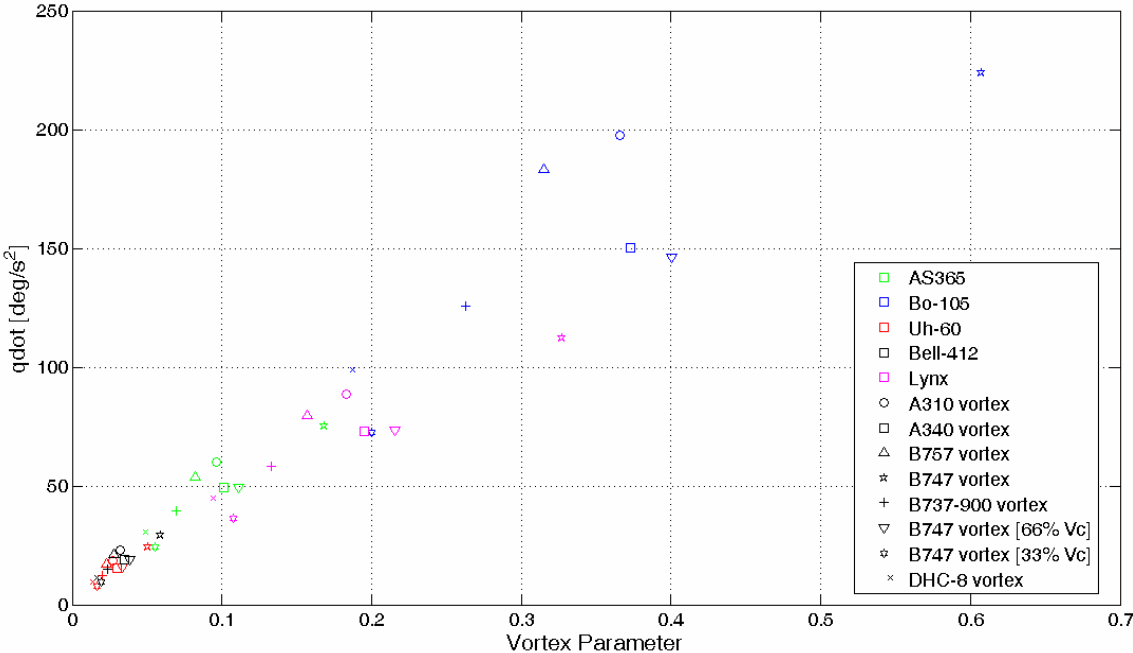


Figure 13 Peak pitch acceleration vs. Vortex Parameter for various rotorcraft-wake vortex combinations (colour indicates r/c type, shape indicates vortex type), V=70kts

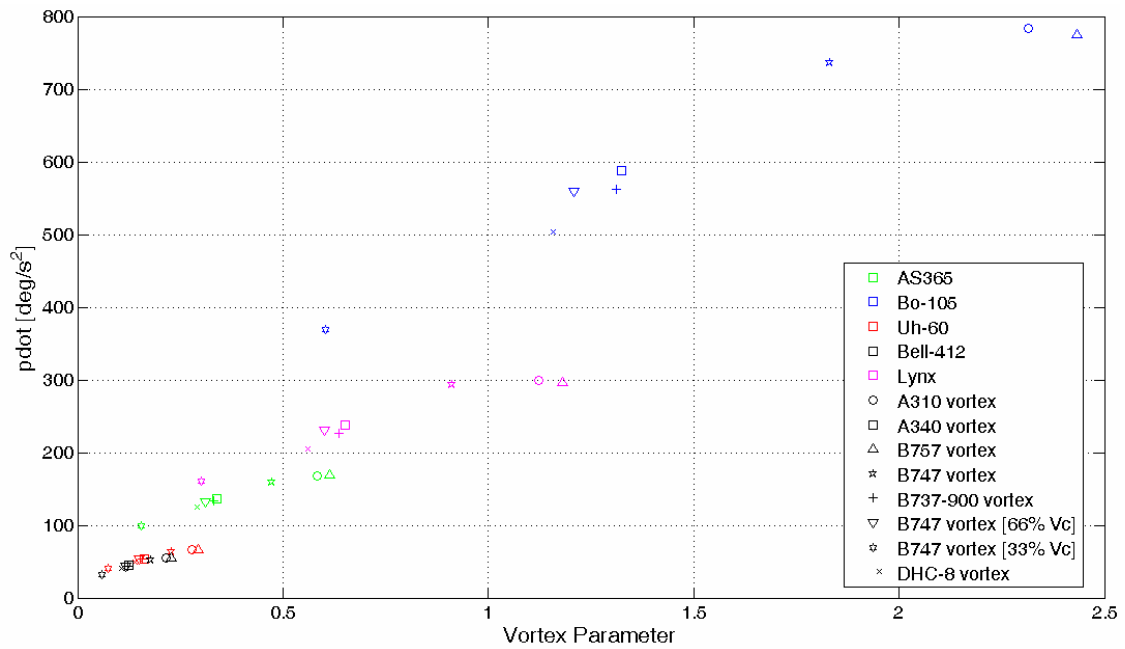


Figure 14 Peak roll acceleration vs. Vortex Parameter= for various rotorcraft-wake vortex combinations (colour indicates r/c type, shape indicates vortex type), $V=70\text{kts}$

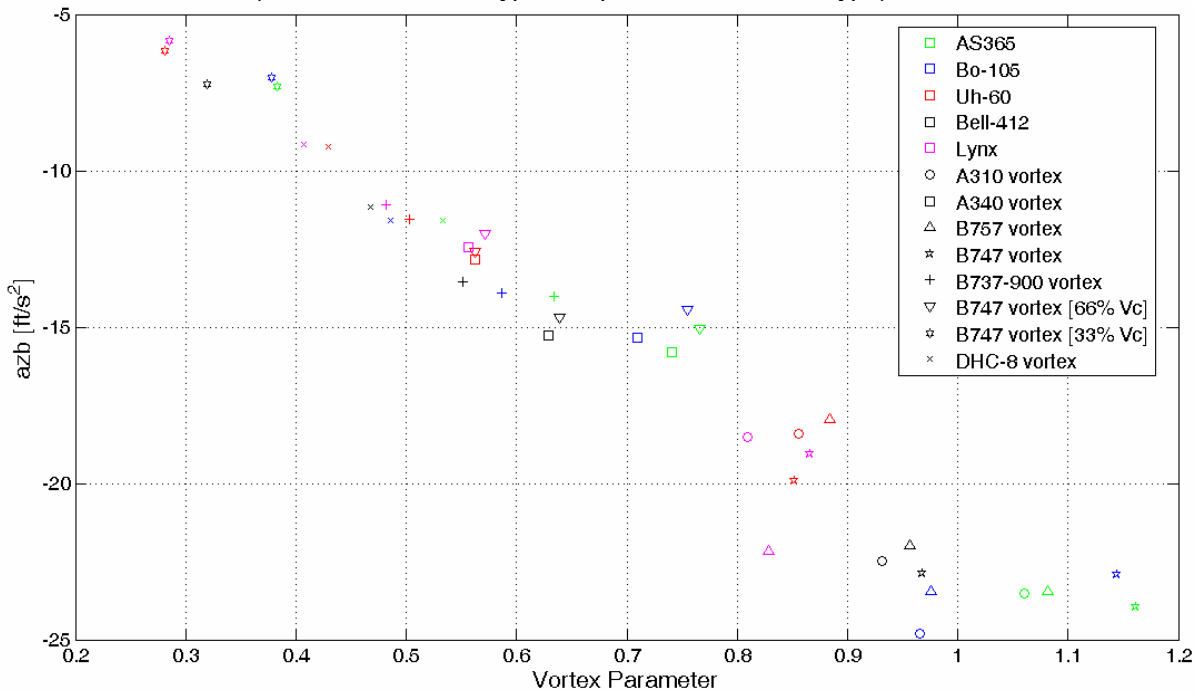


Figure 15 Peak vertical acceleration vs. Vortex Parameter for various rotorcraft-wake vortex combinations (colour indicates r/c type, shape indicates vortex type), $V=70\text{kts}$

The heave axis results are shown in Figure 15 and a better linear correlation is achieved when compared to the angular accelerations. The accelerations range from approximately 5ft/s^2 up to 25ft/s^2 ($0.16g$ to $0.78g$), and the different rotorcraft-wake vortex combinations are spread across the range of results. The ‘Vortex Parameter’ in this case is inversely proportional to the blade loading and proportional to the Vortex core tangential velocity. There is also a contribution that represents the non-linear downwash distribution of the vortex across the rotor disc. It is not surprising that the blade loading works well as part of the Vortex Parameter for this case, as the ride quality, which reflects a rotorcraft’s response to vertical disturbances, is known to be directly linked to the blade loading and subsequently the derivative Z_w .

4.4 Summary of induced acceleration results

A simplified method has been devised to calculate the effect that a particular vortex has on a particular rotorcraft configuration that allows for efficient parametric analyses; fundamental parameters can be adjusted individually to see their effect. Furthermore, the speed of the computation means that many scenarios can be considered quickly and the use of derivative models based on simple input parameters allows easier understanding of the results. However, there are a number of limitations to the approach: the main one is that only the initial quasi-steady acceleration is predicted for a specific orientation and specific location in the vortex. This is useful in giving an indication of the ‘worst-case’ strength of the initial disturbance but the overall ‘severity’ is also dependent on the final displacement caused by an encounter i.e. the attitude upset. Of course, this initial upset is an important factor but the interaction is very much more complex as the rotorcraft moves in time through the vortex. Another is that model is a gross simplification to the real situation – even more so than the non-linear models. Reasonable agreement has been achieved between this method and the non-linear models but nevertheless it is an approximation. The impact of these limitations is that care must be taken in using the results –it is a useful tool for making relative comparisons of the various rotorcraft-wake combinations. Whether the tool can be used to give ‘absolute’ predictions of severity is yet to be established, and requires further investigation.

5 USING THE ANALYTICAL MODEL TO PREDICT SEVERITY

Despite the limitations noted in the previous section, the model had potential for extension and improvement. In particular, the heave axis response was a good candidate for immediate further development. Using the contour analysis results such as in Figures 6-10 it has been found that the induced vertical acceleration is almost independent of flightpath through the vortex (both vertical and lateral). Furthermore, from the piloted tests reported in [12], the vertical response was seen to be reasonably decoupled from the attitude disturbances. In fact, based on the pilot comments and the time histories, it was the vertical response, and thus the vertical flightpath deviations that were often the most important in contributing to high severity ratings and causing ‘go-arounds’. These characteristics opened up the possibility of using a development of the analytical model to consider the overall heave response individually. Also, the opportunity to connect the predicted ‘fast-time’, offline results with the subjective pilot ratings to come up with a severity criterion became a possibility.

5.1 Model Development

There were a number of tasks to be performed to upgrade the model such that the model could compute the complete vertical time response. This required the calculation of the derivative Z_w . Essentially a simple MATLAB state-space model (figure 16) of the form in equation 23 was created to model the single axis response.

$$\dot{x} = Ax + Bu$$
$$\begin{bmatrix} \dot{w} \\ \dot{h} \end{bmatrix} = \begin{bmatrix} Z_w & 0 \\ 1 & 0 \end{bmatrix} \begin{bmatrix} w \\ h \end{bmatrix} + \begin{bmatrix} Z_{\theta_0} \\ 0 \end{bmatrix} \theta_0 \quad (23)$$

The model used inputs such as heading, glideslope, forward speed, starting altitude and lateral position such that a complete trajectory could be modelled and any encounter angle could be investigated. The model also featured a PID controller that can maintain the glideslope for a

basic closed loop analysis. The vortex was modelled by using a scaling factor that adjusts the applied ‘equivalent’ collective as a function of lateral and vertical displacement from the core. This approach is possible due to the fact that the effect of the vortex is more or less independent of the helicopter heading and glideslope. This was ascertained by examination of vortex contours plots as in figures 6-10 for varying glideslopes and heading intercept angles. In the model the attitude perturbations are ignored, the assumption being that the heave responses are fairly independent of the effects of motion in these axes. The scaling factors are pre-calculated and are input to the model via lookup tables. As the helicopter changes position, the scale factor changes and is multiplied by the collective angle calculated using the procedure discussed in section 4.2 of this paper. The scaling factors are based on how the vertical component of the vortex flow changes with position, this being main factor for calculating the heave effect on the rotorcraft. There is some approximation involved as the rotor can be partly within the core where the velocity has linear relationship with distance and partly in the ‘tail’ where there is a logarithmic relationship.

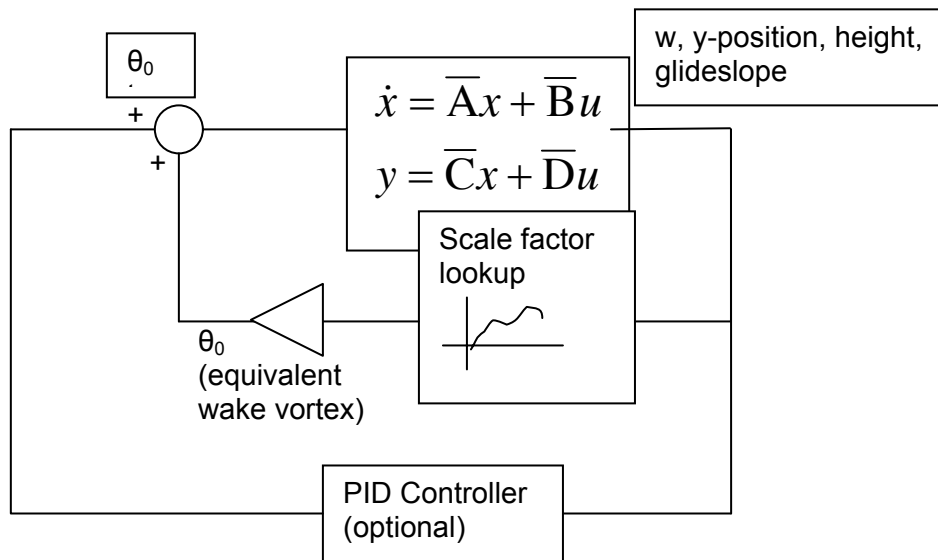


Figure 16 Block Diagram of the MATLAB rotorcraft vertical response model

To check the model, a number of test responses were compared against the non-linear FLIGHTLAB model. Figure 17 shows some example results of a comparison between the vertical response for the non-linear model and the analytically based model flown through a B747 vortex. The flightpath was offset by 20ft to the right of a clockwise vortex such that the helicopter encountered the downwash region of the vortex. Four glideslopes of 3, 6, 9 and 12 degrees are shown in Figure 17 and the vertical acceleration, descent rate and height responses are plotted. There is a good comparison between the two models for all the trajectories with all the flightpaths showing a similar behaviour. It is also interesting to note that the 6 and 9 deg approaches, flown at 60kts and 40kts respectively, are very similar in their descent rate response. This is because the two speed/glideslope combinations have descent rates of approximately 600ft/min, such that they traverse the vortex at the same rate. Furthermore, the derivatives Z_w and Z_{θ_0} don't change much between 60kts and 40kts reinforcing the similarity.

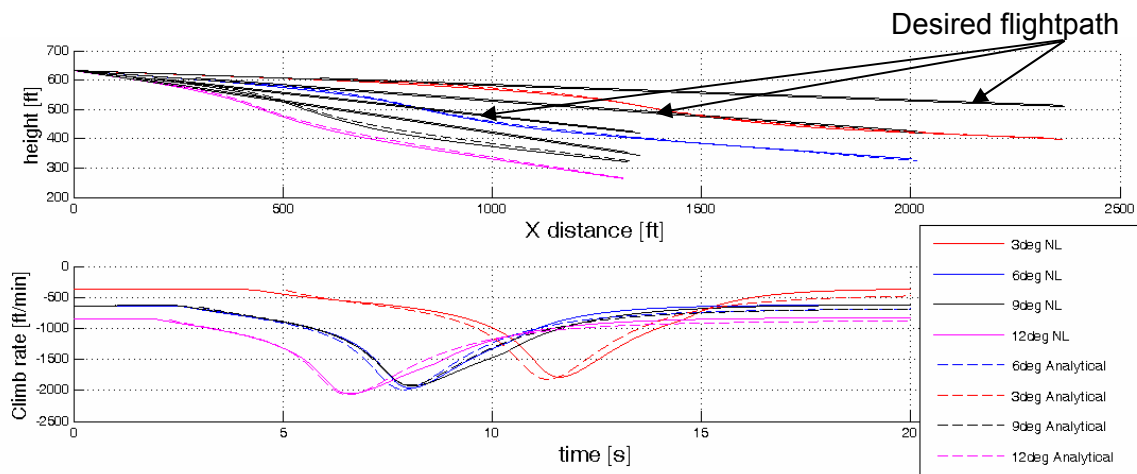


Figure 17 Comparison between the vertical response of a FLIGHTLAB non-linear AS365N helicopter flying through a clockwise B747 and the analytical vortex with an AS365N model

5.2 Comparison with severity ratings

In a previous publication, [12], the main focus for assessing the encounter severity using the ‘Vortex Severity Rating scale’ was the attitude response in the vortex. However, one conclusion was that the vertical response was equally important, if not greater. Of course, the two are linked and Figure 18 shows the average (pitch, roll and yaw combined) peak attitude upsets plotted against peak height deviation from the desired flightpath. The plot shows a trend of increasing attitude upset with increasing height deviation. This makes sense as an increase in vortex strength causes the disturbance to increase in all axes as has been shown in section 4.

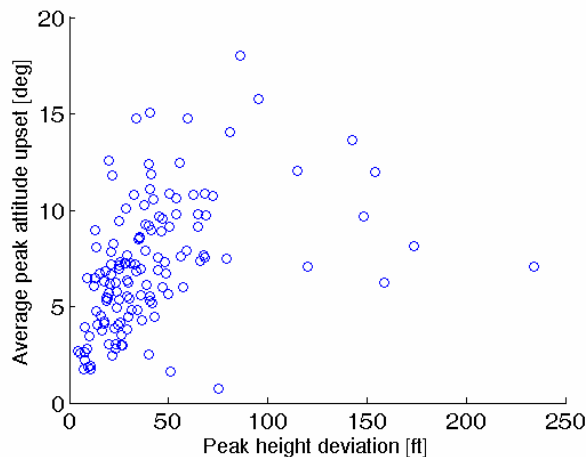


Figure 18 Average peak attitude disturbance (roll, pitch, yaw) versus peak height deviation for various piloted rotorcraft wake vortex encounter simulations

The results in Figure 18 represent a range of scenarios including varying vortex strength, different glideslopes/speeds, varying visual conditions (IMC, VMC) and rotorcraft types (AS365N, FGR, Lynx). All these factors will have an impact on the response and thus the severity rating, but how is severity perceived by the pilot? The underlying idea was that the pilots were adjudging the height perturbation to be critical. In an encounter, this was indicated to a pilot either by high vertical speeds or by the ‘dot’ perturbations of the glideslope indicator. Figure 19 shows the results obtained using the ‘extended’ vertical response model de-

scribed in the previous section. It shows the height perturbations for a range of rotorcraft-wake vortex combinations and for 3 glideslope angles. The rotorcraft are in open-loop mode –again the worst case, with no corrective control being made with respect to the flightpath deviation. Part (a) of Figure 19 is the height perturbation plotted against another ‘Vortex Parameter’ (Equation 25) developed from the similar parameter derived for the vertical acceleration in Figure 15. It was more difficult to achieve a linear correlation as good as in Figure 15 as the height response is dependent on many more parameters than the pure heave acceleration. Furthermore, there is an even more complex relationship with parameters already considered such as rotor radius. The trajectories are shown in (b) of Figure 19 and are for 3deg at 70kts, 6deg at 60kts, and 9deg at 40kts. The scenarios shown are for a parallel encounter, 20ft to the right of a core of a clockwise Boeing 747 vortex. This scenario was selected as it offered the strongest wake vortex and also matched the overall configuration of the piloted simulation scenarios. Note that the linear slope of the perturbations against the Vortex Parameter is fairly independent of glideslope – there is an offset based on vertical rate resulting in the 3° data approximately having a 20ft greater perturbation for any give Vortex parameter.

Height deviation Vortex Parameter:

$$V_c \left(\frac{1}{BL} \right) \left(1 + \exp \left(\frac{r_c}{R} \right) \frac{r_c}{R} \right) \left(\frac{\Omega R}{V} \right) \left(\frac{1}{M_{nd}} \right) \exp \left(\left(\frac{1}{M_{nd}} \right)^2 \left(\frac{\Omega R}{V} \right) \right) \quad (25)$$

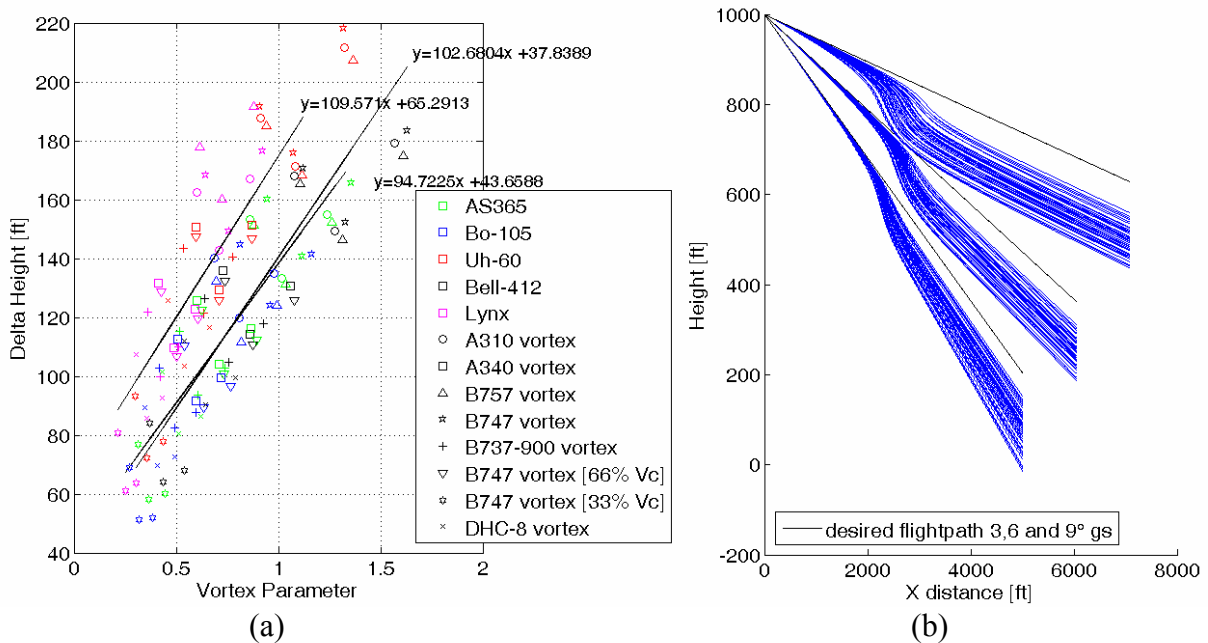


Figure 19 Vortex Parameter vs. Height deviation for various rotorcraft-wake vortex combinations (colour indicates r/c type, shape indicates vortex type)

Figure 20(a) shows the vertical height perturbations plotted against the ‘Vortex Severity Rating’ [12], a linear fit to the mean average of the height deviations for each rating level is also shown. The rating is a subjective score given by the pilot in the range A through to H and is given for two factors, the effect of the vortex, i.e. the magnitude or severity of the disturbances, and the ability to recover from the upset. A is the lowest severity, a hardly detectable disturbance, and H is a catastrophic effect or crash. The ratings are obtained by following a flowchart and the pilot answering several yes-no questions before assigning the rating based

on the best match of descriptors for each severity level. The general trend is an increasing altitude perturbation with increasing severity. The objective was to match this severity to a ‘Vortex Parameter’. One hypothesis was to take the predicted perturbation for a wide range of scenarios and obtain a linear correlation with a Vortex Parameter. Using these two relationships, a Vortex Parameter could be plotted against severity and Figure 20(b) shows results from this approach.

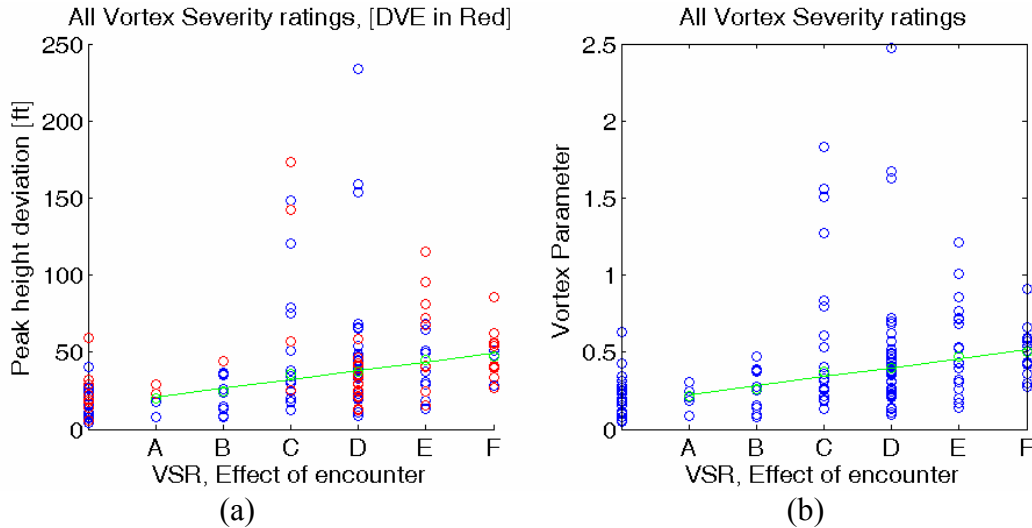


Figure 20 (a) Vortex Severity Rating vs. Height deviation (piloted simulations) (b) Vortex Severity Rating vs. Vortex Parameter (Vortex parameter=94.72*ΔH)

6 DISCUSSION OF ANALYTICAL MODEL ANALYSIS

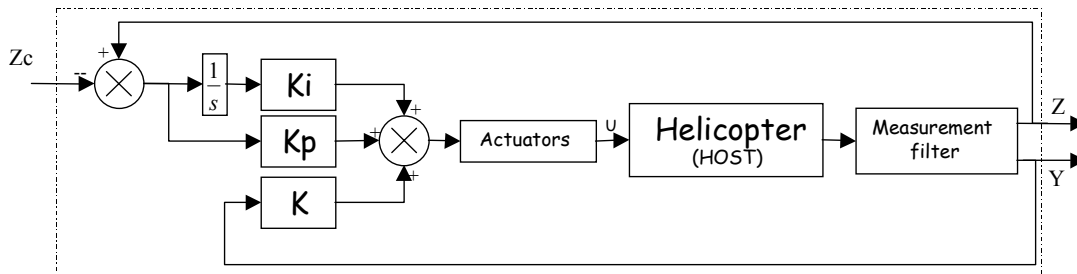
The results have shown how a parameter has been ‘linked’ to severity. Through this type of approach a particular combination of scenario parameters can be approximately ‘risked’ i.e. what is the likely severity of helicopter ‘x’ with vortex ‘y’ in flight condition ‘z’? Admittedly, this correlation is based on many assumptions and a limited dataset but offers a framework and platform for further work. The model could also form the basis for a stochastic Monte Carlo simulation whereby the input parameters are varied randomly within known probability distributions. This could also be linked with vortex transport and decay models and stochastic models of fixed-wing aircraft flightpaths to allow fast-time analysis of ‘real’ SNI proposals. For measuring the severity of the encounters the height deviation based criteria presented here is just one option, another approach could use the predicted initial vertical acceleration. The translational acceleration induced on a rotorcraft is used as a severity measure of a control system failure in ADS-33 [16], this analogy was used in [12] when assessing the attitude upsets. The advantage of using the vertical acceleration is that its prediction has already been shown to be easier than the prediction of the entire flightpath in an encounter. However, whether it is better to use vertical acceleration for vortex encounter severity has still not been determined. The piloted simulations indicated that the vertical flightpath deviations were judged to be most regarding safety. The initial acceleration onset is clearly an integral factor to the height deviation but there are many other factors. For example, two encounters may experience the same peak acceleration but one may have a path that exposes the rotorcraft to a more prolonged disturbance and thus a greater deviation and thus perceived severity. Using height may offer a more generic approach and perhaps is closer to the critical parameter that drives the pilots perceived severity. If such an approach is to be used the correct ‘levels’ have to be set – note that in figure 19 the lowest ‘Delta heights’ (the perturbation from the desired flightpath) were 50ft but these were for open loop responses and cannot be directly

compared to the absolute values shown in Figure 20. Otherwise, all the cases shown in Figure 19 would be deemed high severity because the level ‘F’ encounters were only averaging a 50ft perturbation in the piloted simulation. Clearly, the pilot’s action reduces the perturbation for all the encounters. However, what has been proposed is a method of obtaining a relationship between severity and a height perturbation. What the model currently offers is a relative measure. The lowest severity vs. height deviation is set and the vortex parameter increases from this point based on the ‘known’ relationship with the height deviation from the analytical model. For it to become an ‘absolute’ measure, i.e. for the model to give a measure of the actual loads, disturbances etc of a particular case in isolation, more scenarios have to be considered and more validation has to be conducted.

7 ANALYSIS OF AN AUTOPILOT IN WAKE VORTEX ENCOUNTERS

7.1 Model Development

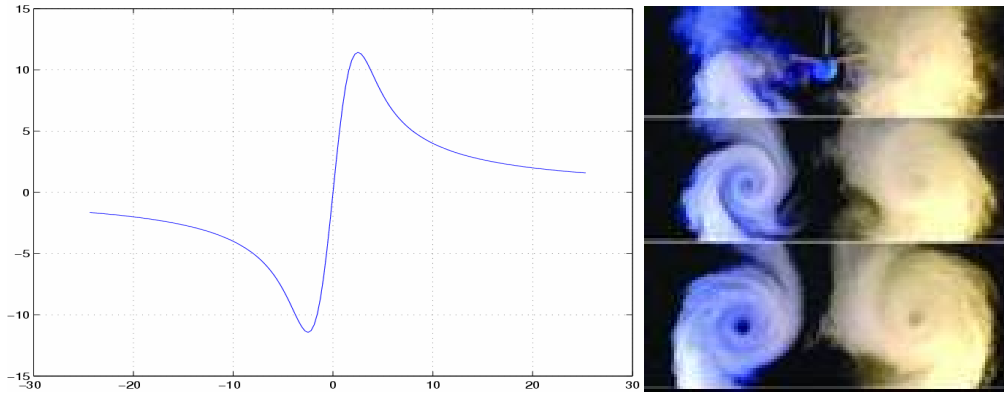
The analytical model presented in the previous sections constitutes a useful instrument for the analysis of the overall mechanism describing the helicopter dynamics in presence of a wake vortex. This work has been augmented using a complimentary approach with the development of a fast time simulation environment. This environment is dedicated to the analysis of the overall helicopter behaviour in various situations of wake vortex interactions. Such analysis should help to estimate, through a set of adequate criteria, the safety distances to respect between the helicopter and the wake vortex core. The fast time simulation environment was developed around EUROCOPTER's flight dynamics code HOST (Helicopter Overall Simulation Tool) [17]. The code was implemented in the MATLAB environment as a "black box". A specific controller was designed to follow a desired descent trajectory. Figure 21 presents the controller inner loop.



$$Z_c = \begin{cases} V_{x_c} & : \text{Targeted } V_x \\ V_{y_c} & : \text{Targeted } V_y \\ V_{z_c} & : \text{Targeted } V_z \\ r_c & : \text{Targeted yaw rate} \end{cases} \quad Y = \begin{cases} p & : \text{Roll rate} \\ q & : \text{Pitch rate} \\ \varphi & : \text{Roll angle} \\ \theta & : \text{Pitch attitude} \end{cases} \quad Z = \begin{cases} V_x & : \text{Ground speed along } X_{\text{body}} \\ V_y & : \text{Ground speed along } Y_{\text{body}} \\ V_z & : \text{Ground speed along } Z_{\text{body}} \\ r & : \text{Yaw rate} \end{cases}$$

Figure 21 Auto-Pilot inner loop

The helicopter model used for this investigation was a Dauphin 365N. The flight dynamics in HOST consisted of a full non linear model using the blade elements to capture the rotor aerodynamics. The wake vortex model was calibrated on a Boeing 747 and modeled as below (Figure 22):



$$V_{\theta}(r) = \frac{V_C \cdot R_C}{r} \left[1 - \exp\left(-\beta_V \left(\frac{r}{R_C}\right)^2\right) \right]$$

Where $\beta_V = 1,2544$

$R_C = 2.51 \text{ m}$; $V_C = 16 \text{ m/s}$

Figure 22 HOST/MATLAB Wake Vortex Model

This model was used to compute the local airspeeds for each helicopter component (horizontal stabilizer, fuselage, tail rotor, blade elements, etc.). Then, these wake vortex airspeeds were applied to each of these components in order to calculate the aerodynamic loads.

7.2 RESULTS

Two simulation cases as shown in Figure 23 are presented. The helicopter mass is 3.8 tonnes and the Vortex generating aircraft's trajectory is in level flight. There is no wake transport model, such as travelling with the wind is applied to the vortices. Therefore, the 2 wake vortices developed behind the aircraft remain fixed in a vertical plane perpendicular to the aircraft flight path. There is also no aging effect which captures the vortices evolution with time. Therefore, the WV model consists of 2 tubes of vortices fixed in space behind the aircraft.

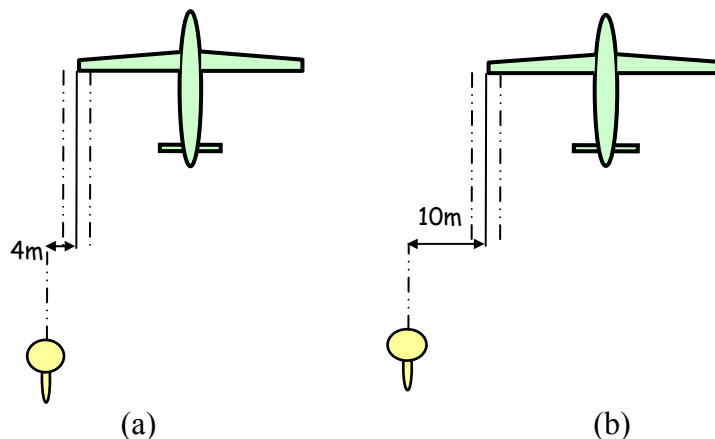
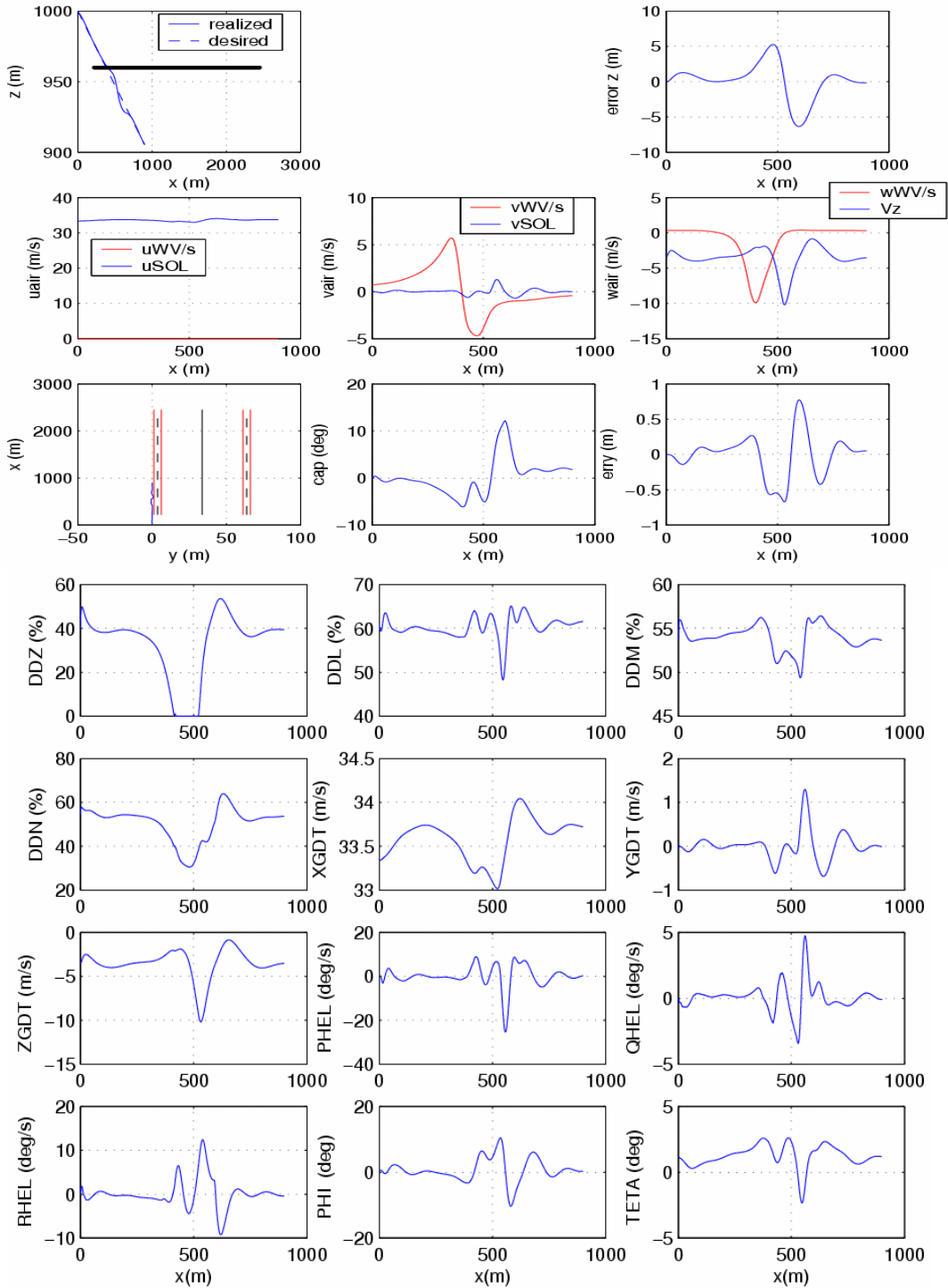


Figure 23 the two example WVE cases for the autopilot analysis

Figures 24 and 25 present a simulation of WVE during a 6° approach angle of the Dauphin at 120 knots. The two vehicles have parallel flightpaths, at the starting point the Dauphin is trimmed at 40m above the aircraft altitude and at a lateral distance of 4m to the left vortex core (figure 23a). The simulation shows a vertical deviation of the flight path from the reference trajectory, first up by 5m due to the initial upwash in the wake and then down by 6m. A collective saturation was noted during the recovery phase (Figure 24, DDZ).



x,y,z	: helicopter positions in earth axes
errorz, erry	: Vertical and lateral deviations from the reference trajectory
uWV/s, vWV/s, wWV/s	: Longitudinal, lateral and vertical airspeeds in the WV, in body axes
uSOL, vSOL	: Helicopter longitudinal and lateral ground speeds in body axes
Vz	: Helicopter vertical ground speed in body axes
Cap	: Heading
DDZ, DDL, DDM, DDN	: Collective, lateral and longitudinal Cyclic and the pedals
XGDT, YGDT, ZGDT	: Helicopter longitudinal and lateral and vertical ground speeds in body axes
PHEL, QHEL, RHEL	: Roll, pitch and yaw rates
PHI, TETA	: Bank angle, pitch angle

Figure 24 Time histories, 6deg approach, parallel flightpaths, 4m lateral separation (B747 vortex)

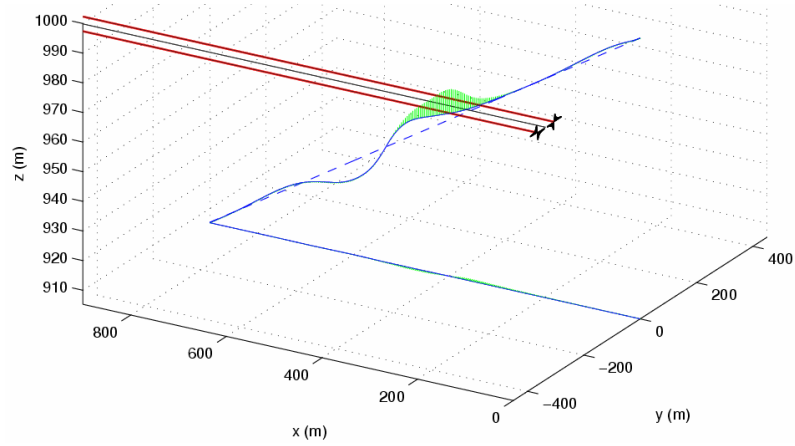


Figure 25 3D trajectory 6deg approach, parallel flightpaths, 4m lateral separation (B747 vortex)

Table 2 summarises the deviations from the reference trajectory during the recovery and the required pilot control activity. Note the relatively high controller range of travel (53% collective, 35% pedals (min to max input)) in order to recover the reference trajectory. During the encounter the helicopter passes through the upwash region of the vortex requiring the collective to go to its lower limit. This kind of control saturation could cause problems during a descent close the ground.

$\Delta\Psi$ (deg)	ΔZ (m)	ΔY (m)	ΔCol (%)	$\Delta long$ (%)	Δlat (%)	Δped (%)	V_{zmax} (m/s)	D recover (m)
+12	+5.2	+0.8	+15	+2	+5	+10	-10	500
-6	-6.4	-0.7	-38	-5	-12	-25		

Table 2 Control and positional displacements in 6deg, parallel WVE (4m lateral displacement, B747 vortex)

Figures 26 and 27 present the same simulation with a lateral distance to the vortex core of 10m (Figure 23b). At this distance, the velocities of the wake vortex are much less than in the previous case. At 4m distance, the lateral wind speed was fluctuating around +/-5m/s and the vertical wind speed was between 0 and -10m/s. At 10m distance these values become respectively between +/-2m/s in lateral and 0 to -4m/s in vertical.

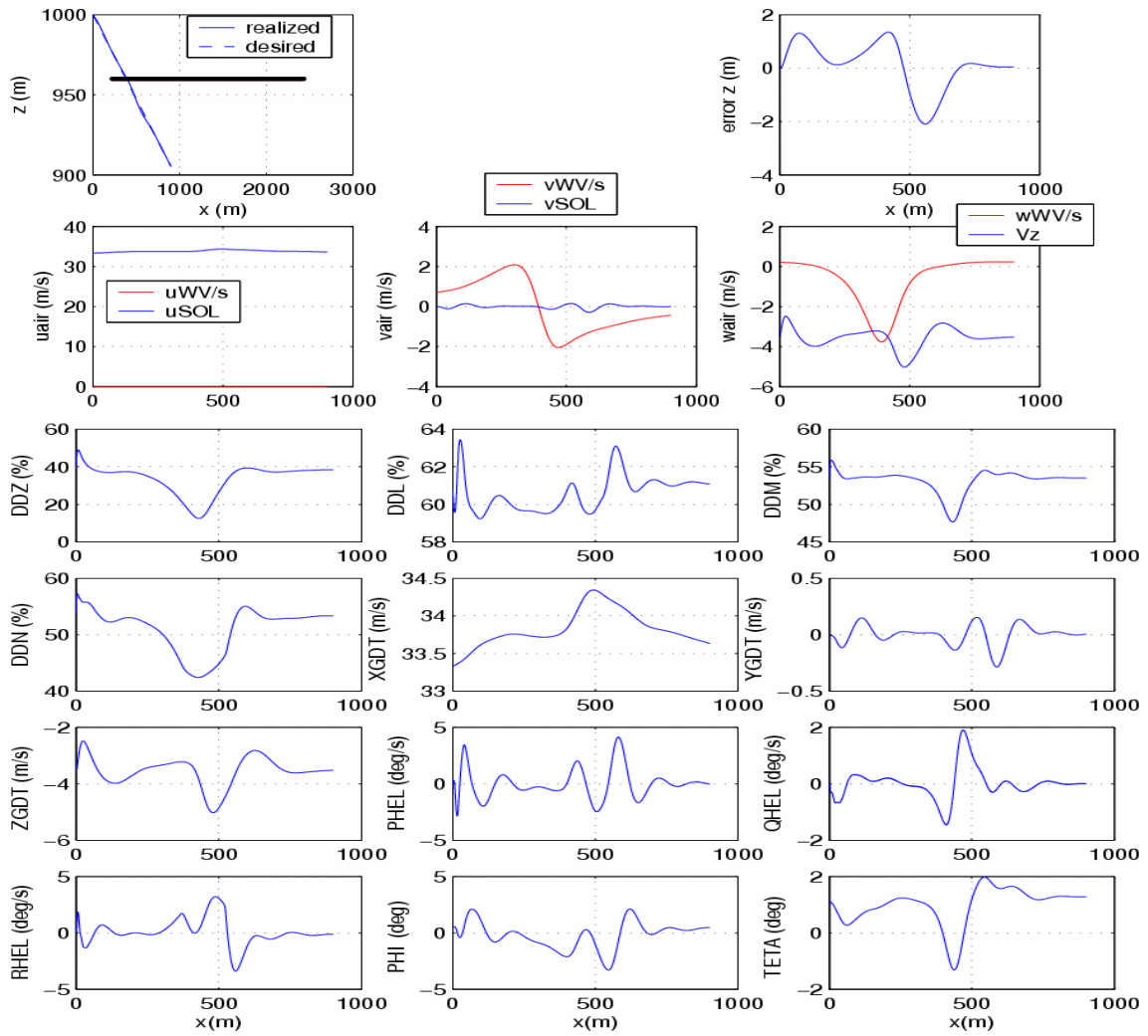


Figure 26 Time histories, 6deg approach, parallel flightpaths, 10m lateral separation (B747 vortex)

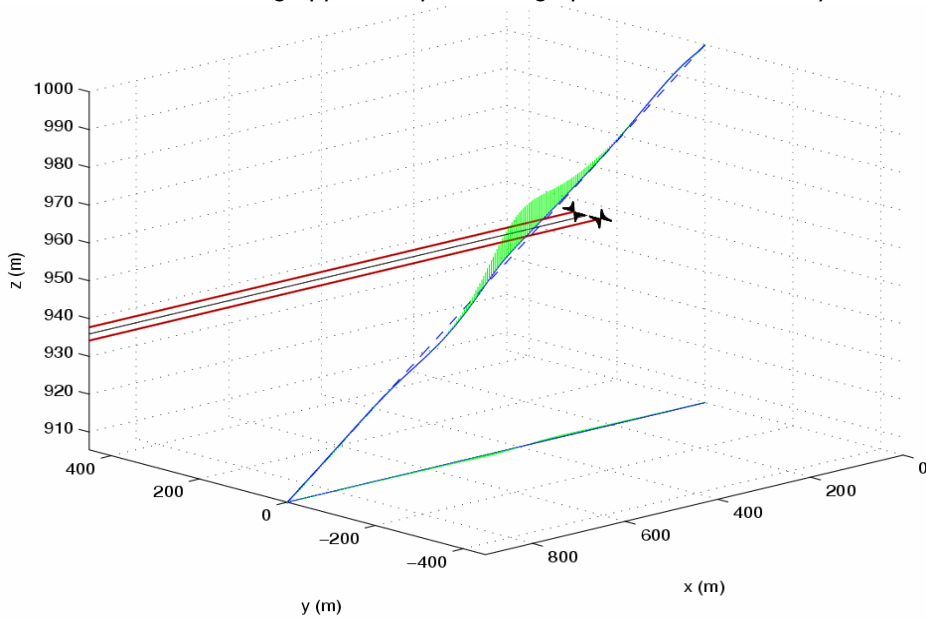


Figure 27 3D trajectory 6 deg approach, parallel flightpaths, 10m lateral separation (B747 vortex)

Table 3 gives a comparison of the typical deviations between the 2 cases. The pilot control activity seems acceptable for the second case except on the collective stick where it reaches a maximum deviation of 25%.

	$\Delta\Psi$ (deg)	ΔZ (m)	ΔY (m)	ΔCol (%)	$\Delta long$ (%)	Δlat (%)	Δped (%)	Vzmax (m/s)	D recover (m)
10m to the WV core	+9 -1	+1.3 -2.1	+0.1 -0.3	0 -25	0 -6	+4 0	+2 -10	-5	600
4m to the WV core	+12 -6	+5.2 -6.4	+0.8 -0.7	+15 -38	+2 -5	+5 -12	+10 -25	-10	500

Table 3 Control and positional displacements in 6deg, parallel WVE (10m lateral displacement, B747 vortex)

7.3 DISCUSSION ON THE AUTOPILOT MODEL METHODOLOGY

The investigations using the autopilot model have provided the typical trajectory deviations and the corresponding pilot activity for recovering. A series of criteria based around these types of deviations could be defined in order to select the "unsafe approach cases". These criteria should be defined using pilots and operators experience. Again the axis that is of most concern is the vertical response, and the collective control has been shown to reach saturation in trying to correct for the disturbance. Finally, a particular attention should be given to the case of OEI (One Engine Inoperative) procedures. During a landing approach, helicopters may encounter a failure on one engine. Below, the so-called LDP altitude (Landing Decision Point) they must demonstrate their capability to land using only one engine. However, due to the reduction of the available engine power (50%) they operate close to the flight envelope limits (particularly on vertical axis). Encountering a wake vortex in this situation could have catastrophic consequences. Therefore, specific investigations should be carried out in order to define the acceptable level of wake vortex perturbations below the LDP. If such a procedure is not realisable in presence of wake vortex, then no wake vortex encounter should be accepted within a certain (as yet unspecified) proximity to the ground.

8 CONCLUSIONS

This paper has shown how a linear velocity distribution analogy has been used to develop a simplified rotorcraft/fixed-wing wake vortex encounter model. In the development of this model a greater understanding of the aeromechanics of wake vortex encounters has been obtained. The key conclusions from this analysis are:

1. Processes have been defined for 'synthesizing' how the peak roll, pitch, yaw and heave accelerations are induced for the 'worst cases' of the parallel wake encounter scenario. For the acceleration predictions, the method has been able to achieve variable levels of agreement with the non-linear models but have consistent trends.
2. Relationships have been developed between the analytical model and various 'Vortex parameters' that incorporate various key factors of the rotorcraft, vortex and trajectory and resulting acceleration. These parameters could be used to 'predict' the rotorcraft response in particular encounters and give an indication of the severity.

3. Using results from previous piloted simulations, a correlation between attitude perturbation and severity has been established; this representation has been applied to the vertical flight path disturbance and a correlation between severity and height perturbations shown.
4. Using the height perturbation relationship an analytical model was developed to calculate the entire descent trajectory through a wake vortex encounter. This model featured the ability to model different trajectories, vortices, and any conventional rotorcraft. This model was also used to develop a relationship between height deviation from a desired glideslope and the Vortex Parameter that represented a particular encounter.
5. An approach using an autopilot model has been developed which predicts typical trajectory deviations and the corresponding pilot activity for recovery. As a result, a series of criteria based around these types of deviations could be defined in order to select the 'unsafe approach' threshold.

Although some initial correlations have been established this research is still regarded as 'work-in-progress' and there are a few caveats to be aware of. These include the limited number of scenarios used, scatter in pilot ratings and the number of simplifying assumptions within the modelling. The way that the data from the piloted experiments has been applied has been fairly simplistic, taking ratings from tests that featured varying vortex strengths, glideslopes, rotorcraft types and visual conditions. However, notwithstanding those factors, it is suggested that perceived severity vs. height deviation is fairly independent of all the other variables except perhaps the effects of flying in poor visibility. In summary, a measure of severity is likely to depend on a number of factors such as height and attitude displacements, angular rates and accelerations induced, or the control inputs required to recover. It is too early to be able to say definitively which metrics should be incorporated for any severity analysis, but a number of options have been proposed with tentative proposals for where the levels should be. The realm of handling qualities analysis is offering useful guides to how to approach the question of severity through the severity rating scale drawing analogy with a control system failure causing a transient upset. More development is required to consolidate the methods and metrics proposed through a process of model validation and dialogue with operators and pilots. The approximate models presented in this paper should be developed to include more cases and could possibly lead to a model that incorporates the full six-degree-of-freedom response. However, maintaining the feature that the models are based on stability and control derivatives derived from simple design parameter inputs is an important aspect. This enables a simple and effective method for the comparison of the fundamental design parameters with the wake encounter response. These kinds of models can then be extended to include the wind effect on the wake vortex transport to assess individual airport cases, in order to define the safe distances between aircraft runways and the FATO. The critical issue here is primarily safety, but without being over prescriptive or over-conservative such that the new operations are excessively compromised. Throughout the model development process many simplifications have been made and a key question remains concerning the validity of the superposition of velocities assumption. This is the basis of the more 'complex' non-linear models which the analytical models are verified against. There is still no definitive research existing that establishes the validity of the superposition principle, pointing to the need for further research to assess this through experimental or CFD methods.

9 ACKNOWLEDGEMENTS

This work has been conducted on behalf of the European Commission Framework VI project 'OPTIMAL'. Thanks are also given to the test pilots Andy Berryman, Nigel Talbot and Steve Cheyne who flew the simulation trials.

10 REFERENCES

- [1] Anon, "European Aeronautics: A Vision for 2020," European Commission, Luxembourg: Office for Official Publications of the European Communities, 2001.
- [2] Sawyer, B. M., Peisen, D. J., and Reuss, L. M., "Simultaneous and Non-Interfering (SNI) Rotorcraft Operations," Vol. SAIC/TR 99-01, Science Applications International Corporation, Arlington, VA, 1999.
- [3] Sammonds, R. I. and Stinnet Jr., G. W., "Criteria relating Wake Vortex Hazard to Aircraft Response," *Journal of Aircraft*, Vol. 14, No. 10, 1977, pp. 981-986.
- [4] Gerz, T., Holzäpfel, F., Darracq, D., de Bruin, A., Elsenaar, A., Speijker, L., Harris, M., Vaughan, M., and Woodfield, A. A., "Aircraft Wake Vortices: A Position Paper," 2001.
- [5] Mantay, W. R., Holbrook, G. T., Campbell, R. L., and Tomaine, R. L., "Helicopter Response to an Airplane's Trailing Vortex," *Journal of Aircraft*, Vol. 14, No. 4, 1977, pp. 357-362.
- [6] Azuma, A., Kawachi, K., and Okuno, Y., "Study of the Dynamic Response of Helicopters to a Large Airplane Wake," 12th European Rotorcraft Forum, Garmisch-Partenkirchen, Germany, 1986.
- [7] Saito, S., Azuma, A., Okuno, Y., and Hasegawa, T., "Numerical Simulations of Dynamic Response of Fixed and Rotary Wing Aircraft to a Large Airplane Wake," 13th European Rotorcraft Forum, Arles, France, 1987.
- [8] Azuma, A., Saito, S., and Kawachi, K., "Response of a Helicopter Penetrating the Tip Vortices of a Large Airplane," *Vertica*, Vol. 11, No. 1/2, 1987, pp. 65-76.
- [9] Padfield, G. D. and Turner, G. P., "Helicopter encounters with aircraft vortex wakes," *Raes Aeronautical Journal*, Vol. 105, No. 1043, 2001, pp. 1-8.
- [10] Turner, G. P., Padfield, G. D., and Harris, M., "Encounters with Aircraft Vortex Wakes: The Impact on Helicopter Handling Qualities," *Journal of Aircraft*, Vol. 39, No. 5, 2002.
- [11] Padfield, G. D., Manimala, B., and Turner, G. P., "A Severity Analysis for Rotorcraft Encounters with Vortex Wakes," *Journal of the American Helicopter Society*, 2004, pp. 445-456.
- [12] Lawrence, B. and Padfield, G. D., "Wake vortex Encounter Severity for Rotorcraft in Approach and Landing," 31st European Rotorcraft Forum, Florence, Italy, 2005.
- [13] DuVal, R. W., "A Real-time Multi-Body Dynamics Architecture for Rotorcraft Simulation," "The Challenge for Realistic Simulation", RAeS Conference, London, 2001.
- [14] Padfield, G. D., *Helicopter Flight Dynamics*, 1st ed., Blackwell Science, Oxford, 1996.
- [15] Lawrence, B. and Padfield, G. D., "Wake Vortex Encounter Severity for Rotorcraft in Approach and Landing," 31st European Rotorcraft Forum, Florence, Italy, 2005.
- [16] Anon, "Aeronautical Design Standard: Performance Specification; Handling Qualities for Military Rotorcraft," Vol. ADS-33E-PRF, United States Army Aviation and Missile Command, Aviation Engineering Directorate, Redstone Arsenal, Alabama, USA, 2000.
- [17] Benoit, B., Dequin, A.-M., Basset, P.-M., Gimonet, B., Von Grunhagen, W., and Kampa, K., "HOST: A General Helicopter Simulation Tool for Germany and France," 56th American Helicopter Society Forum, Virginia Beach, VA, 2000.